

Tidal Charged Black Holes as Particle Accelerators to Arbitrarily High Energy

Parthapratim Pradhan,^a

^a*Department of Physics,
Vivekananda Satabarshiki Mahavidyalaya
(Vidyasagar University),
Manikpara, West Midnapur,
West Bengal-721513, India.*

E-mail: pppradhan77@gmail.com

ABSTRACT: We show that Randall Sundrum tidal charged spherically symmetric vacuum brane black holes could be act as a particle accelerator with ultrahigh center-of-mass energy in the limiting case of *maximal black hole tidal charge*. For non-extremal Randall Sundrum tidal charged black hole, the center-of-mass energy is finite. While for maximally Randall Sundrum tidal charged black hole, the center-of-mass energy is *infinite*. We have also derived the center-of-mass energy at ISCO (Innermost Stable Circular Orbit) or LSCO (Last Stable Circular Orbit) or MSCO (Marginally Stable Circular Orbit) and MBCO (Marginally Bound Circular Orbit) for maximally Randall Sundrum tidal charged black hole. We show visually the differences between Reissner-Nordström black hole and Randall Sundrum tidal charged BH. We have found that for maximally Randall Sundrum tidal charged black hole the center-of-mass energy is satisfied the following inequality: $E_{cm}|_{r_+} > E_{cm}|_{r_{mb}} > E_{cm}|_{r_{ISCO}}$ i.e. $E_{cm}|_{r_+=\frac{M}{M_p^2}} : E_{cm}|_{r_{mb}=(\frac{3+\sqrt{5}}{2})\frac{M}{M_p^2}} : E_{cm}|_{r_{ISCO}=4\frac{M}{M_p^2}} = \infty : 3.23 : 2.6$. Which is exactly *similar* to the spherically symmetric extreme Reissner-Nordström black hole.

¹Corresponding author.

Contents

1	Introduction	1
2	RS Tidal Charged BH metric and its Properties:	3
3	Equatorial circular orbit in the RS Tidal charged BH:	7
3.1	Particle Case:	9
3.2	Photon Case:	12
3.3	MBCO:	15
3.4	ISCO:	15
4	CM Energy of Particle Collision near the horizon of the RS Tidal charged BH:	16
5	CM Energy of Particle Collision near the Horizon of a non-Extremal RN BH:	27
6	Summary and Outlook:	30

1 Introduction

In 2009, Bañados, Silk and West(BSW) have argued that when two massive dark matter particles falling freely from rest to exterior of an extremal Kerr black hole(BH), it could be act as a natural particle accelerators with an infinite amounts of center-of-mass(CM) energy[1]. Whereas in case of non-spinning Schwarzschild BH, this CM energy is found to be finite i.e. $E_{cm} = 2\sqrt{5}m_\chi$, where m_χ is the mass of the two colliding particles[2].

It has been pointed out by Berti et al.[4] and Jacobson[5], to produce such arbitrarily high CM energy it is indeed require exactly an extremal BH and an extremal event horizon etc.. Any deviation from maximally situations, the CM energy is also reduced to the order of less than ten times the mass of the colliding particles. In [4], the authors proposed that there should be some astrophysical practical limitations i.e. maximal spin, back reaction effect, gravitational radiation and sensitivity to the initial conditions etc. on that CM energy due to the Thorn's bound[6] i.e. $\frac{a}{M} = \frac{J}{M^2} = 0.998$ (where M is the mass and a is the spin of the BH).

There were numerous studies have been done by different authors for different BHs on account of BSW mechanism. Particularly, Lake [10] argued that the CM energy at the Cauchy horizon(\mathcal{H}^-) of a static Reissner-Nordström (RN) BH and Kerr BHs are limited. Grib and Pablov [11] investigated the CM energy using the multiple scattering process. Also in [12], the same authors derived the CM energy of particle collisions in the ergo-sphere

of the Kerr BH. The collision in the ISCO particles were investigated by the Harada et al.[13] for Kerr BH. Liu et al. [14] studied the BSW effect for Kerr-Taub-NUT(Newman, Unti, Tamburino) space-time and proved that the CM energy depends upon both the Kerr parameter (a) and the NUT parameter (n) of the space-time. In [15], the authors showed that the Kerr-AdS BH space-time could be act as a particle accelerator. Studies were done by [16] for RN-de-Sitter BH and found that infinite energy in the CM frame near the cosmological horizon. The authors in [17] investigated the particle accelerations and collisions in the back ground of a cylindrical BHs. Studies of BSW effect were done in [18] for the naked singularity case of different space-times.

In [19], the authors elucidated the CM energy for the Kerr-Newman BH. For Kerr-Sen BH, the CM energy is diverging also computed in [20]. It was derived in [21] regarding the BSW effect for charged BH. The authors in [22] discussed that general stationary charged BHs as particle accelerators. In [23], the author showed a weakly magnetized BH behaves as a particle accelerators. Mc-Williams [24] proved that the BHs are neither particle accelerators nor dark matter probes. The author in [25] also investigated that the CM energy in the context of the near horizon geometry of the extremal Kerr BHs and proved that the CM energy is finite for any value of the particle parameters. Tursunov et al. [26] showed the particle accelerations and collisions in case of black string. In [3], the authors attempted to compute the escape fraction and the flux at infinity of the highly blue shifted dark-matter particles. In [7], the authors proposed that using collisional Penrose process the emitted massive particles can only be gain ~ 30 percentage of the initial rest energy of the in-falling particles.

More recently, Schnittman[8] computed a new upper limit on the energy that could be extracted from an extremal Kerr BH in the ergo-sphere by means of collisional Penrose process. Berti et al.[9] showed particle collisions in the vicinity of Kerr BHs can produce arbitrarily high efficiencies by means of “super-Penrose” process.

BH solutions arises not only in general relativity and string theory, but also in brane-world gravity models. There has been many brane-world models with extra dimensions in which the standard model fields live on a three-brane and only gravity propagate in the bulk[30–34, 36]. Such large extra spatial dimensions and TeV scale quantum gravity may open up the possibility that microscopic BHs could be produced and detected at the CERN Large Hadron Collider(LHC)[35, 36]. Thus it is important to investigate all of the implications of the Randall-Sundrum models[32] for particle accelerators. A class of Randall-Sundrum(RS) solutions have been found in which the solution is a RN metric with the electric charge replaced by a *tidal charge*. Now we will called it RS tidal charged BH[37].

In the present work, we wish to investigate the BSW mechanism for RS tidal charged spherically symmetric BHs characterized by their mass(M) and tidal charge (q) localized on a three-brane in 5D gravity in the Randall-Sundrum scenario. For $q > 0$, they are formally identical to the RN BH of general theory of relativity. Thus the CM energy is diverging for the *extremal* case. For $q < 0$, there exists only one horizon then the CM energy is finite. Lastly for $M = 0$ and $q < 0$, we get the CM energy is also finite. Firstly, we present the complete geodesic structure of the RS tidal charged BH. Then we derived the ISCO, MBCO and CPO of the said BH. Finally, we compute the CM energy at various

collision points say ISCO, MBCO etc. and show that at the horizon the E_{cm} is maximum than the MBCO and ISCO for extremal RS tidal charged BH which is the analogue of the extremal RN BH. We prove that for extreme RS tidal charged BH the ratio becomes $E_{cm}|_{r_+=\frac{M}{M_p^2}} : E_{cm}|_{r_{mb}=\left(\frac{3+\sqrt{5}}{2}\right)\frac{M}{M_p^2}} : E_{cm}|_{r_{ISCO}=4\frac{M}{M_p^2}} = \infty : 3.23 : 2.6$, which is exactly similar to the extremal RN BH. In fact it suggests that $E_{cm}|_{r_+} > E_{cm}|_{r_{mb}} > E_{cm}|_{r_{ISCO}}$.

The paper is organized as follows. In section 2, we shall study the basic characteristics of tidal charged BH. In section 3, we shall explained clearly the complete geodesic structure of the said BH. Section 4 will devoted to study the CM energy of the RS tidal charged BH. Section 5 will discussed the CM energy for RN BH. Finally, we conclude our discussions in section 6.

2 RS Tidal Charged BH metric and its Properties:

The metric of a static, spherically symmetric RS tidal charged BH[33] is given by

$$ds^2 = -\mathcal{B}(r)dt^2 + \frac{dr^2}{\mathcal{B}(r)} + r^2(d\theta^2 + \sin^2\theta d\phi^2) . \quad (2.1)$$

where the function $\mathcal{B}(r)$ is defined by

$$\mathcal{B}(r) = \left(1 - \frac{2M}{M_p^2 r} + \frac{q}{M_5^2 r^2}\right) . \quad (2.2)$$

where M is defined as the BH mass, q is the dimensionless tidal charge, $M_p (= 1.2 \times 10^{16} Tev)$ is the effective Plank mass on the brane and M_5 is the fundamental Planck scale in the 5D bulk. It should be noted that the above metric is nearly identical to the RN metric (5.1), except that the RN term $\frac{Q^2}{r^2}$, which is necessarily non-negative, is replaced by $\frac{q}{M_5^2 r^2}$ that can have any sign. In Fig.1, we show how the metric coefficient changes for RS tidal charged BH in contrast with RN BH. From the figure, it is clear that the change of metric coefficients look similar both for RS tidal charged BH and RN BH in the extremal limit i.e. $q = Q = 1$.

Eq. (2.1) is an exact solution of effective Einstein equation on the brane i.e.

$$G_{ab} = -\Lambda g_{ab} + \frac{8\pi}{M_p^2} T_{ab} + \left(\frac{8\pi}{M_5^3}\right)^2 S_{ab} - \mathcal{E}_{ab} . \quad (2.3)$$

where,

$$M_p = \sqrt{\frac{3}{4\pi}} \left(\frac{M_5^2}{\sqrt{\lambda}}\right) M_5, \quad (2.4)$$

$$\Lambda = \frac{4\pi}{M_5^3} \left[\Lambda_5 + \left(\frac{4\pi}{3M_5^3}\lambda^2\right)\right], \quad (2.5)$$

$$\Lambda_5 = -\frac{4\pi\lambda^2}{3M_5^3}. \quad (2.6)$$

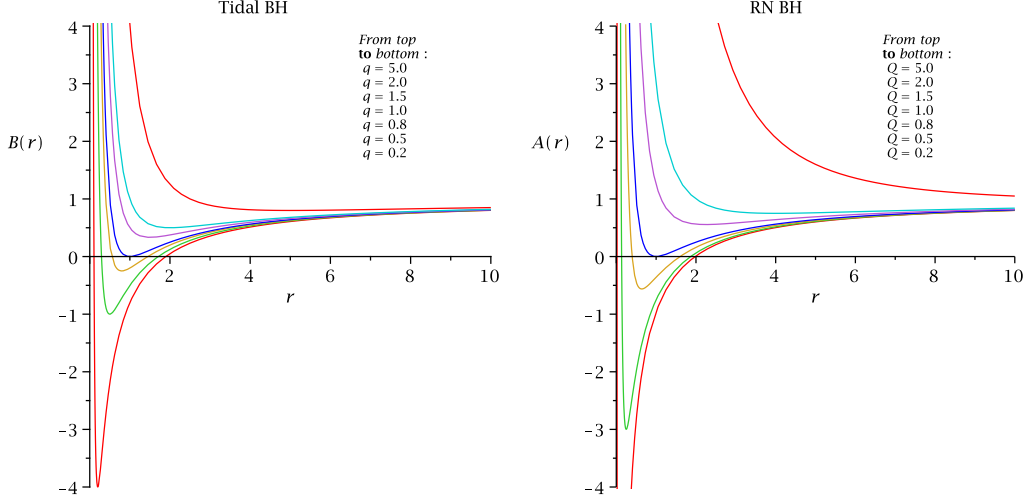


Figure 1. The figure shows the variation of g_{tt} with r for Brane-world BH and RN BH with $M = M_p = M_5 = 1$.

Generally, $M_5 \ll M_p$ i.e. the fundamental Planck scale is much lower than the effective scale in the brane-world. For the vacuum case, it should be noted that $T_{ab} = S_{ab} = 0 = \Lambda$. Then Eq.(2.3) is reduced to

$$R_{ab} = -\mathcal{E}_{ab}, R_a^a = 0 = \mathcal{E}_a^a. \quad (2.7)$$

Now the four dimensional horizon structure of the RS tidal charged BH strictly depends on the sign of q .

Case I: When $q \geq 0$, then the component $g_{tt} = 0$ gives two horizons:

$$r_{\pm} = \frac{M}{M_p^2} \left[1 \pm \sqrt{1 - \frac{qM_p^4}{M^2 M_5^2}} \right], \quad (2.8)$$

which is analogous to the spherically symmetric RN BH. Here r_+ and r_- are called event horizon (\mathcal{H}^+) or outer horizon and Cauchy horizon (\mathcal{H}^-) or inner horizon respectively. The $r_+ = r_-$ or $M^2 = q \left(\frac{M_p^4}{M_5^2} \right)$ corresponds to the extremal case and in this case the extremal horizon is situated at

$$r_+ = r_- = \frac{M}{M_p^2}. \quad (2.9)$$

Since in general theory of relativity(GTR), both horizons lie inside the Schwarzschild horizon i.e. $0 \leq r_- \leq r_+ \leq r_s = \frac{2M}{M_p^2}$, and there is an upper bound on q i.e. $0 \leq q \leq q_{max} = \left(\frac{M_5}{M_p} \right) \left(\frac{M}{M_p} \right)^2$.

We observe that the event horizon and Cauchy horizons are qualitatively different both for RS tidal charged BH and RN BH, which can be seen from Fig. 2.

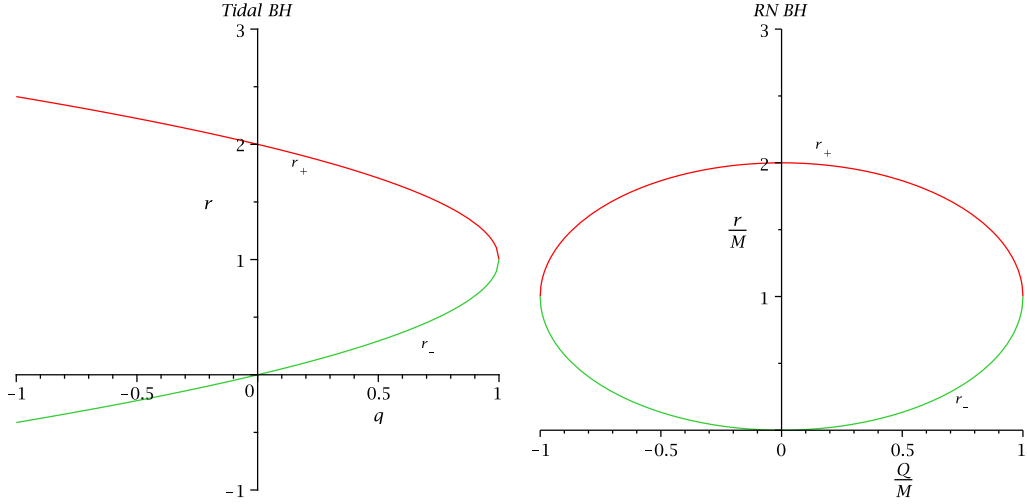


Figure 2. The figure shows the qualitative behavior of horizons for RS tidal charged BH and RN BH with $M = M_p = M_5 = 1$.

Case II: When $q < 0$, which is impossible in GTR RN case leads to single horizon, lying exterior to the Schwarzschild horizon:

$$r_+ = \frac{M}{M_p^2} \left[1 + \sqrt{1 - \frac{qM_p^4}{M^2M_5^2}} \right] > r_s, \quad (2.10)$$

Case III: When $M = 0$ and $q < 0$, in this case the metric becomes

$$ds^2 = - \left[1 + \frac{q}{M_5^2 r^2} \right] dt^2 + \frac{dr^2}{\left[1 + \frac{q}{M_5^2 r^2} \right]} + r^2 (d\theta^2 + \sin^2 \theta d\phi^2) \quad (2.11)$$

The horizon still exists without the gravitational sources and on the brane it is given by

$$r_+ = \frac{\sqrt{-q}}{M_5}. \quad (2.12)$$

This implies that in the absence of gravitational collapse of matter, there is an intriguing possibility of string tidal effects in the early universe could lead to BH formation. Then the tidal charge q would be determined by both the brane source i.e. the mass M , and any coulomb part of the bulk. Weyl tensor that survives when M is set to be zero. Now we shall discuss shortly the thermodynamic properties of tidal charged BH. In Figs. (3, 4, 5, 6), we show the differences between RS tidal charged BH and RN BH from the thermodynamical point of view.

The surface gravity of \mathcal{H}^\pm for the tidal charged BH is given by

$$\kappa_\pm = \pm \frac{\sqrt{(\frac{M}{M_p^2})^2 - \frac{q}{M_5^2}}}{2(\frac{M}{M_p^2})r_\pm - \frac{q}{M_5^2}}. \quad (2.13)$$

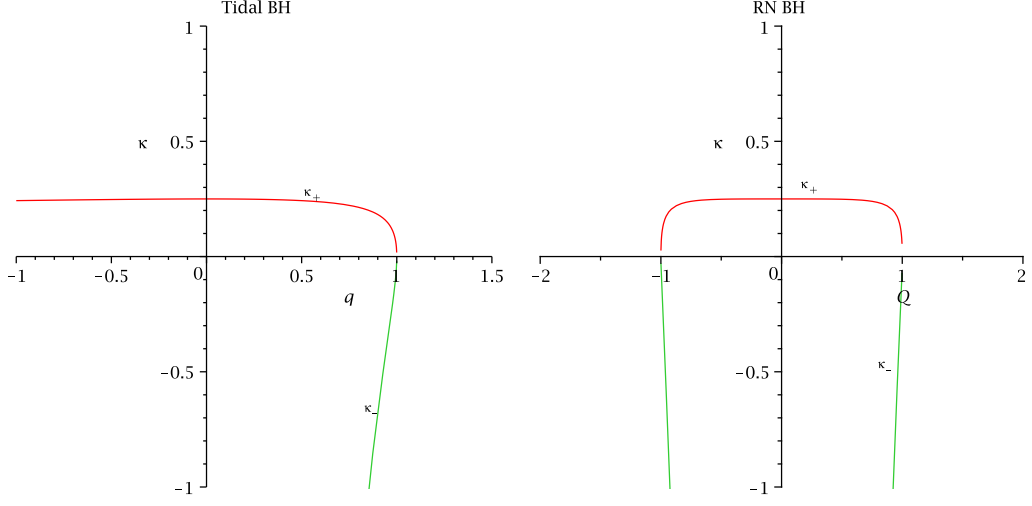


Figure 3. The figure shows the qualitative behavior of surface gravity for RS tidal charged BH and RN BH while $M = M_p = M_5 = 1$.

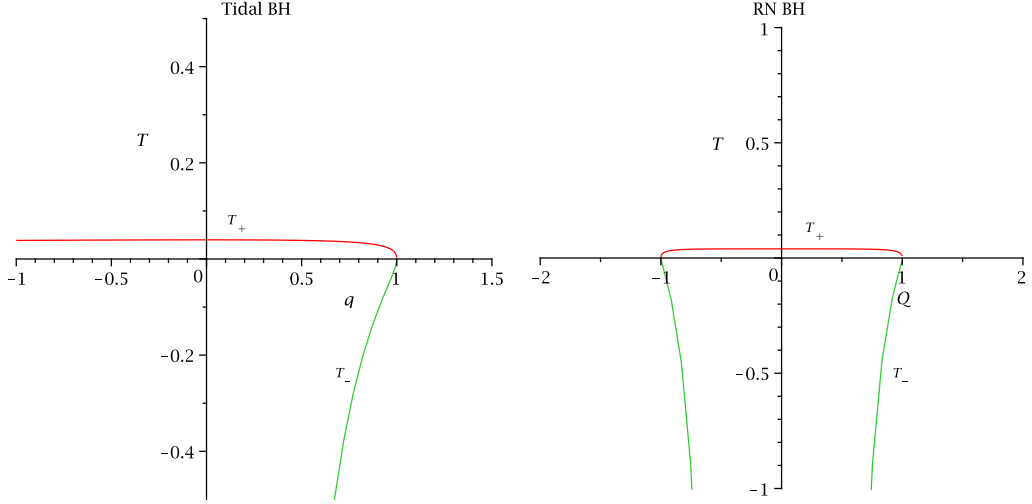


Figure 4. The figure depicts the qualitative behavior of Hawking temperature for RS tidal charged BH and RN BH while $M = M_p = M_5 = 1$.

Similarly, the BH temperature or Hawking temperature of \mathcal{H}^\pm is

$$T_\pm = \pm \frac{\sqrt{(\frac{M}{M_p^2})^2 - \frac{q}{M_5^2}}}{2\pi[2(\frac{M}{M_p^2})r_\pm - \frac{q}{M_5^2}]} . \quad (2.14)$$

Then the area of both the horizons (\mathcal{H}^\pm) are

$$\mathcal{A}_\pm = 4\pi[2(\frac{M}{M_p^2})r_\pm - \frac{q}{M_5^2}] . \quad (2.15)$$

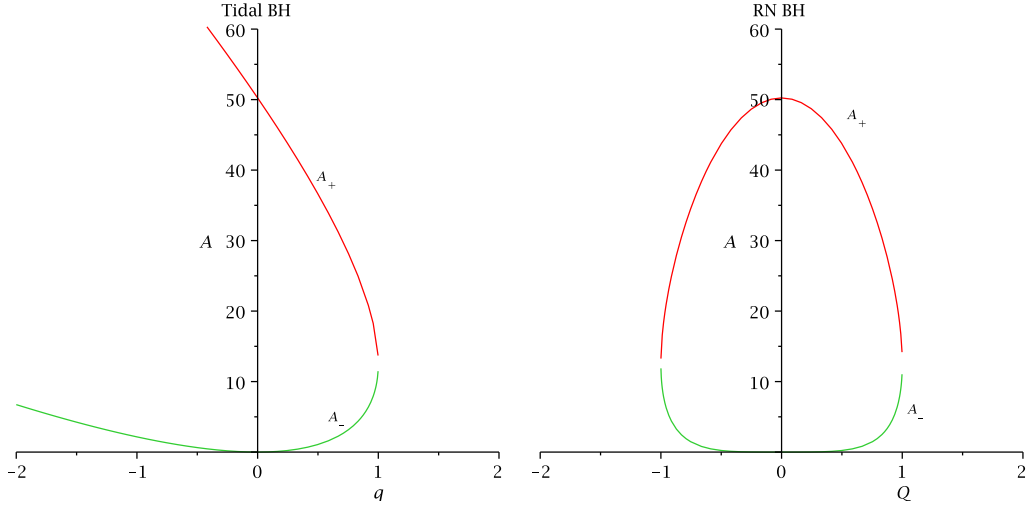


Figure 5. The figure shows the qualitative behavior of surface area for RS tidal charged BH and RN BH while $M = M_p = M_5 = 1$.

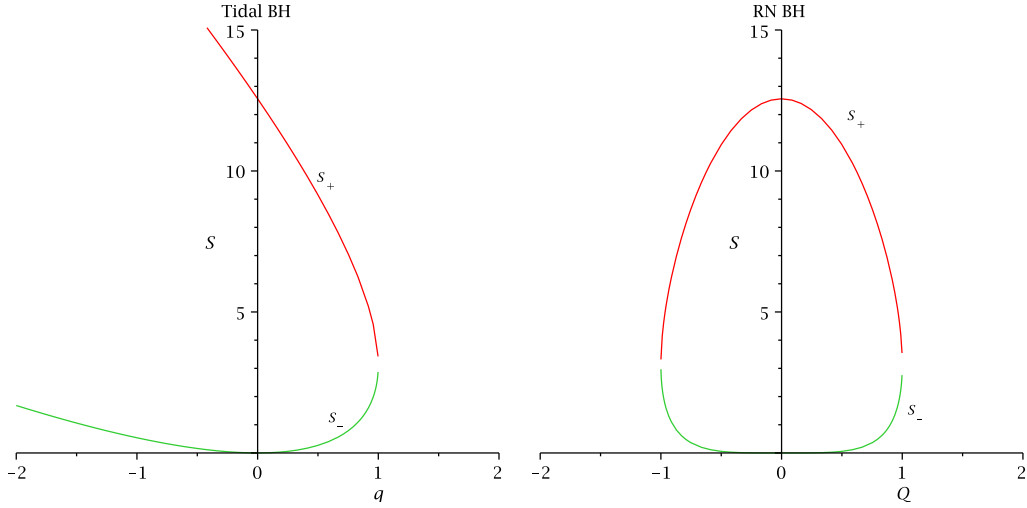


Figure 6. The figure shows the qualitative behavior of entropy for RS tidal charged BH and RN BH while $M = M_p = M_5 = 1$.

Finally, the entropy of \mathcal{H}^\pm is

$$\mathcal{S}_\pm = \frac{\mathcal{A}_\pm}{4} = \pi \left[2 \left(\frac{M}{M_p^2} \right) r_\pm - \frac{q}{M_5^2} \right]. \quad (2.16)$$

3 Equatorial circular orbit in the RS Tidal charged BH:

To derive the CM energy, first we need to know in detail the complete geodesic structure of the brane-world BH in the equatorial plane i.e. $\theta = \frac{\pi}{2}$. We also compute ISCO or MSCO or

LSCO, MBCO and CPO of the said BH. They are very crucial in BH accretion disk theory. To determine the geodesic motion of a test particle in the equatorial plane we impose the condition i.e. $u^\theta = \dot{\theta} = 0$ and $\theta = \text{constant} = \frac{\pi}{2}$ and follow the well known book of S. Chandrasekhar[29]. Therefore we can write the Lagrangian in terms of the metric is given by

$$\mathcal{L} = \frac{1}{2} \left[-\mathcal{B}(r) \dot{t}^2 + \frac{\dot{r}^2}{\mathcal{B}(r)} + r^2 \dot{\phi}^2 \right] . \quad (3.1)$$

Now the generalized momenta could be derived from Lagrangian reads

$$p_t \equiv \frac{\partial \mathcal{L}}{\partial \dot{t}} = -\mathcal{B}(r) \dot{t} . \quad (3.2)$$

$$p_r \equiv \frac{\partial \mathcal{L}}{\partial \dot{r}} = (\mathcal{B}(r))^{-1} \dot{r} . \quad (3.3)$$

$$p_\theta \equiv \frac{\partial \mathcal{L}}{\partial \dot{\theta}} = r^2 \dot{\theta} = 0 . \quad (3.4)$$

$$p_\phi \equiv \frac{\partial \mathcal{L}}{\partial \dot{\phi}} = r^2 \dot{\phi} . \quad (3.5)$$

Here superior dots denote differentiation with respect to affine parameter which is the proper time (τ) for massive particles and for massless particles it is affine parameter(λ).

Since the Lagrangian density does not depend explicitly on the variables ' t ' and ' ϕ ', so p_t and p_ϕ are conserved quantities. Thus one obtains,

$$p_t = -\mathcal{B}(r) \dot{t} = -E = \text{constant} . \quad (3.6)$$

$$p_\phi = r^2 \dot{\phi} = L = \text{constant} . \quad (3.7)$$

Solving (3.6) and (3.7) for \dot{t} and $\dot{\phi}$ we get

$$\dot{t} = \frac{E}{\mathcal{B}(r)} . \quad (3.8)$$

$$\dot{\phi} = \frac{L}{r^2} . \quad (3.9)$$

where E and L are the energy per unit mass and angular momentum per unit mass of the test particle.

The normalization of the four velocity(\mathbf{u}) gives another integral equation for the geodesic motion:

$$\mathbf{u} \cdot \mathbf{u} = \epsilon . \quad (3.10)$$

or

$$-E \dot{t} + L \dot{\phi} + \frac{1}{\mathcal{B}(r)} \dot{r}^2 = \epsilon . \quad (3.11)$$

Here, $\epsilon = -1$ for time-like geodesics, $\epsilon = 0$ for light-like geodesics and $\epsilon = +1$ for space-like geodesics.

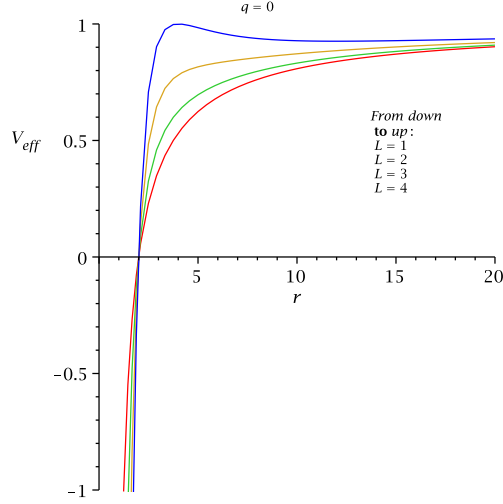


Figure 7. The figure depicts the variation of V_{eff} with r for RS tidal charged BH in the limit $q = 0$ with $M = M_p = M_5 = 1$.

Substituting the equations, (3.8) and (3.9) in (??), we get the radial equation that governs the complete geodesic structure of RS tidal charged BH is given by

$$\dot{r}^2 = E^2 - V_{eff} = E^2 - \left(\frac{L^2}{r^2} - \epsilon \right) \mathcal{B}(r) . \quad (3.12)$$

where, the standard effective potential for brane-world BH would become

$$V_{eff} = \left(\frac{L^2}{r^2} - \epsilon \right) \mathcal{B}(r) . \quad (3.13)$$

3.1 Particle Case:

For massive particles, the effective potential becomes

$$\begin{aligned} V_{eff} &= \left(1 + \frac{L^2}{r^2} \right) \left(1 - \frac{r_+}{r} \right) \left(1 - \frac{r_-}{r} \right) \\ &= \left(1 + \frac{L^2}{r^2} \right) \left(1 - \frac{2M}{M_p^2 r} + \frac{q}{M_5^2 r} \right) . \end{aligned} \quad (3.14)$$

Figs. (7, 8, 9, 10) describes the qualitative differences between RS tidal charged BH and RN BH in the effective potential for various values of angular momentum. Note that the structure of the effective potential is exactly same in the extremal limit both for tidal charged BH and RN BH that can be seen from Fig. 10.

In the extremal limit, the effective potential(See Fig. 10) is found to be

$$V_{eff} = \left(1 + \frac{L^2}{r^2} \right) \left(1 - \frac{r_+}{r} \right)^2 . \quad (3.15)$$

For circular geodesic motion of the test particle of constant $r = r_0$, one obtains

$$V_{eff} = E^2 . \quad (3.16)$$

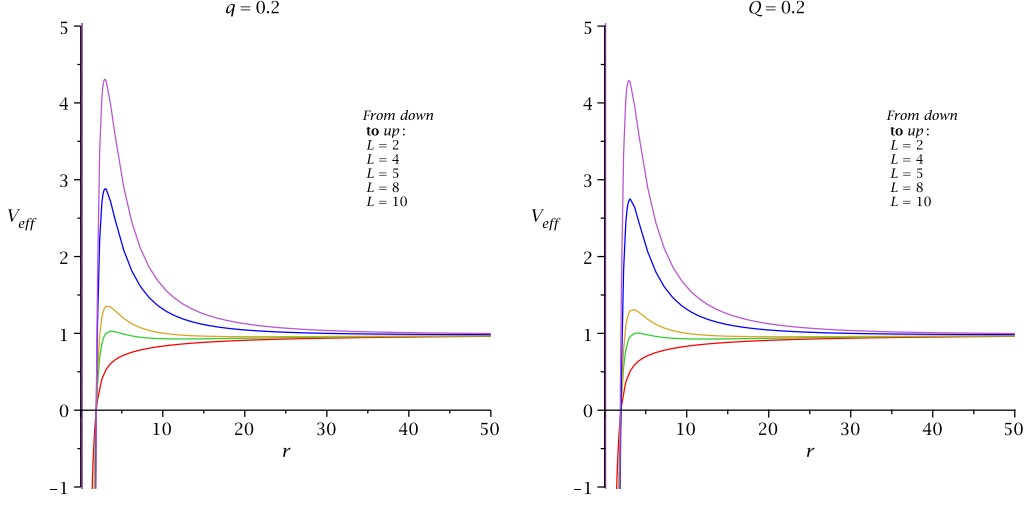


Figure 8. The figure shows the variation of V_{eff} with r for RS tidal charged BH and RN BH with $M = M_p = M_5 = 1$.

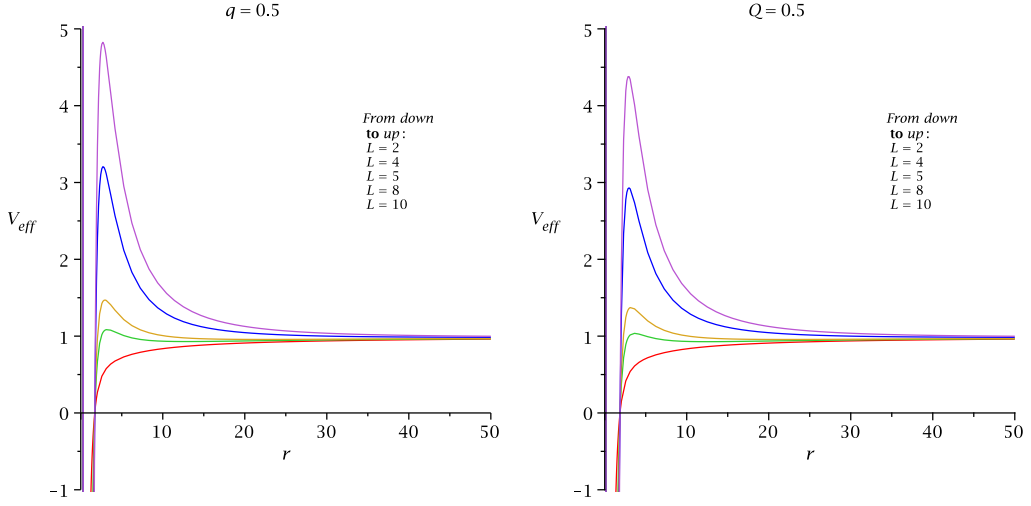


Figure 9. The figure shows the variation of V_{eff} with r for RS tidal charged BH and RN BH with $M = M_p = M_5 = 1$.

and

$$\frac{dV_{eff}}{dr} = 0 . \quad (3.17)$$

Therefore we obtain the conserved energy per unit mass and angular momentum per unit mass of the test particle along the circular orbits:

$$E_0^2 = \frac{2(r_0 - r_+)^2(r_0 - r_-^2)}{r_0^2[2r_0^2 - 3(r_+ + r_-)r_0 + 4r_+r_-]} . \quad (3.18)$$

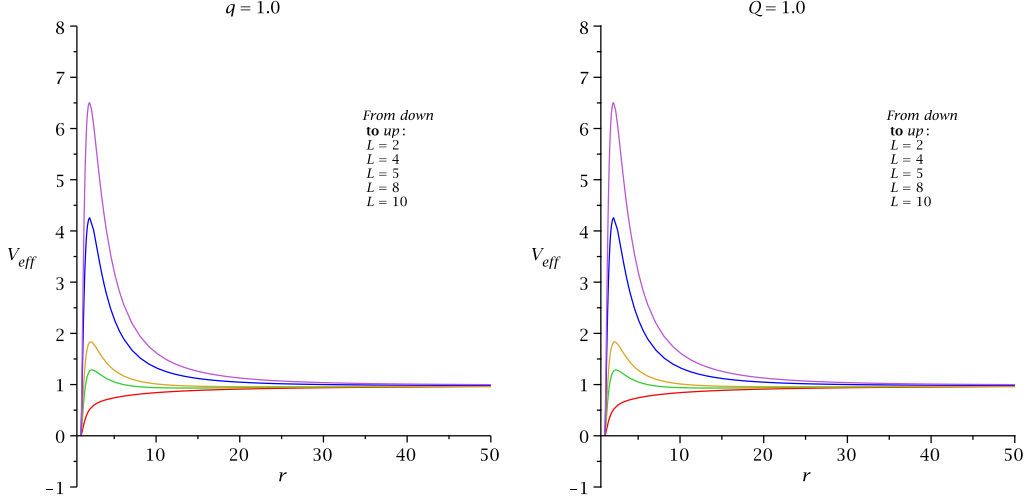


Figure 10. The figure shows the variation of V_{eff} with r for RS tidal charged BH and RN BH in the extremal limit i.e. $q = Q = 1$ with $M = M_p = M_5 = 1$.

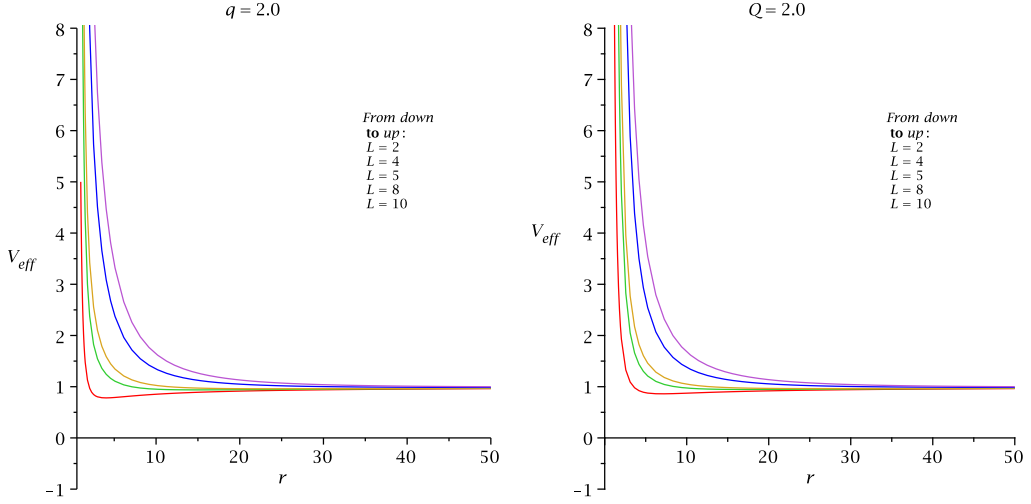


Figure 11. The figure shows the variation of V_{eff} with r for RS tidal charged BH and RN BH with $M = M_p = M_5 = 1$.

and

$$L_0^2 = \frac{r_0^2[r_0(r_+ + r_-) - 2r_+r_-]}{2r_0^2 - 3(r_+ + r_-)r_0 + 4r_+r_-} . \quad (3.19)$$

For our record, we also note the energy and angular momentum for extremal tidal charged BH reads as

$$E_0^2 = \frac{(r_0 - r_+)^3}{r_0^2(r_0 - 2r_+)} . \quad (3.20)$$

and

$$L_0^2 = \frac{r_0^2 r_+}{r_0 - 2r_+} . \quad (3.21)$$

Circular motion of the test particle to be exists when both the energy and angular momentum are real and finite. Thus one obtains,

$$2r_0^2 - 3(r_+ + r_-)r_0 + 4r_+r_- > 0 \text{ and } r_0 > 2\frac{r_+r_-}{r_+ + r_-} . \quad (3.22)$$

General relativity does not permit arbitrary circular radii, so the denominator of equations (3.18,3.19) real only if $2r_0^2 - 3(r_+ + r_-)r_0 + 4r_+r_- \geq 0$. The limiting case of equality gives circular orbit with infinite energy per unit mass, i.e. a circular photon orbit(CPO). This photon orbit is the innermost boundary of the circular orbit for massive particles.

Comparing the above equation of particle orbits with (3.30) when $r_0 = r_c$, we can see that photon orbit is the limiting case of time-like circular orbit. It occurs at the radius

$$r_c = r_{cpo} = \frac{1}{4} \left[3(r_+ + r_-) \pm \sqrt{9(r_+ + r_-)^2 - 32r_+r_-} \right] . \quad (3.23)$$

In the extremal limit, one obtains

$$r_{cpo} = 2r_+ = 2r_- = 2\frac{M}{M_p^2} . \quad (3.24)$$

3.2 Photon Case:

For massless particles, the effective potential would become

$$\begin{aligned} U_{eff} &= \frac{L^2}{r^2} \mathcal{B}(r) = \frac{L^2}{r^2} \left(1 - \frac{r_+}{r} \right) \left(1 - \frac{r_-}{r} \right) \\ &= \frac{L^2}{r^2} \left(1 - \frac{2M}{M_p^2 r} + \frac{q}{M_5^2 r} \right) . \end{aligned} \quad (3.25)$$

In Figs. (12,13,14,15) we show how the effective potential U_{eff} changes for different values of angular momentum L for two BHs.

In the extremal limit, one gets

$$U_{eff} = \frac{L^2}{r^2} \mathcal{B}(r) = \frac{L^2}{r^2} \left(1 - \frac{r_+}{r} \right)^2 . \quad (3.26)$$

For circular null geodesics at $r = r_c$, one gets

$$U_{eff} = E^2 . \quad (3.27)$$

and

$$\frac{dU_{eff}}{dr} = 0 . \quad (3.28)$$

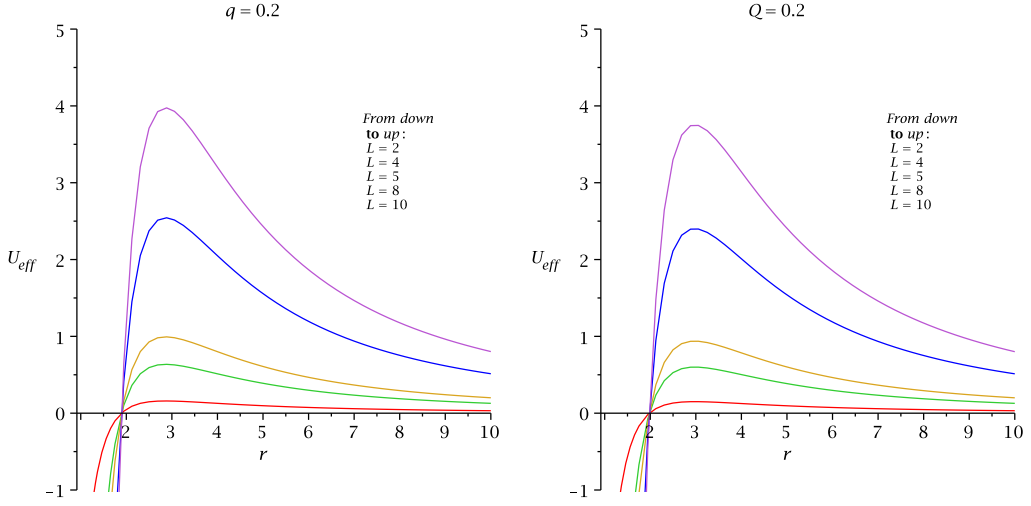


Figure 12. The figure shows the variation of U_{eff} with r for RS tidal charged BH and RN BH with $M = M_p = M_5 = 1$.

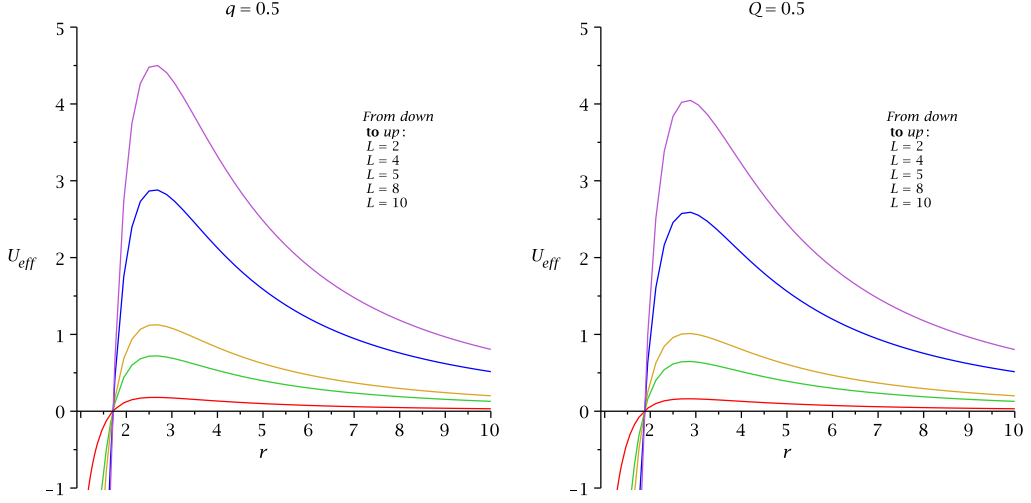


Figure 13. The figure shows the variation of U_{eff} with r for RS tidal charged BH and RN BH with $M = M_p = M_5 = 1$.

Therefore one can evaluate the ratio of energy and angular momentum of the test particle evaluated $r = r_c$ for CPO

$$\frac{E_c}{L_c} = \frac{\sqrt{(r_c - r_+)(r_c - r_-)}}{r_c^2}. \quad (3.29)$$

and

$$2r_c^2 - 3(r_+ + r_-)r_c + 4r_+r_- = 0. \quad (3.30)$$

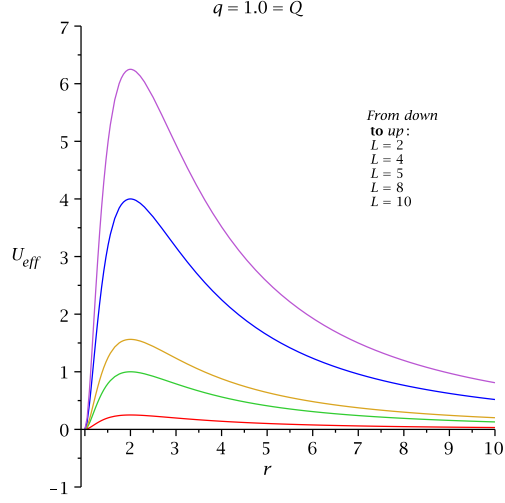


Figure 14. The figure shows the variation of U_{eff} with r for RS tidal charged BH and RN BH in the extremal limit with $M = M_p = M_5 = 1$.

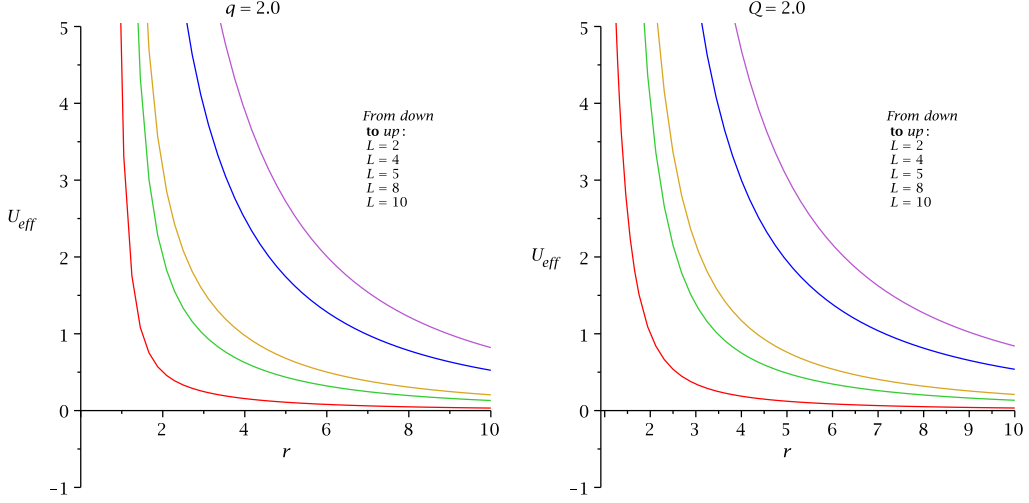


Figure 15. The figure shows the variation of U_{eff} with r for RS tidal charged BH and RN BH with $M = M_p = M_5 = 1$.

Let $r_c = r_{cpo}$ be the solution of the Eq.(3.30) which gives the radius of the CPO of the brane-world BH.

After introducing the impact parameter $D_c = \frac{L_c}{E_c}$, the above equation could be re-written as

$$\frac{1}{D_c} = \frac{E_c}{L_c} = \frac{\sqrt{(r_c - r_+)(r_c - r_-)}}{r_c^2} = \Omega_c . \quad (3.31)$$

where Ω_c is the angular frequency.

In the extremal limit $r_+ = r_-$, this could be reduced to

$$\Omega_c = \frac{1}{D_c} = \frac{E_c}{L_c} = \frac{(r_c - r_+)}{r_c^2} . \quad (3.32)$$

Now the classical capture cross-section is given by

$$\sigma = \pi D_c^2 = \pi \frac{r_c^4}{(r_c - r_+)(r_c - r_-)} . \quad (3.33)$$

In the extremal limit this would be

$$\sigma_{ex} = \pi D_c^2 = \pi \frac{r_c^4}{(r_c - r_+)^2} . \quad (3.34)$$

3.3 MBCO:

Another important class of orbit is the MBCO could be found by setting $E_0^2 = 1$ in Eq. (3.18), then we get the MBCO equation:

$$(r_+ + r_-)r_0^3 - 2(r_+ + r_-)^2 r_0^2 + 4r_+ r_- (r_+ + r_-)r_0 - 2(r_+ r_-)^2 = 0 . \quad (3.35)$$

or

$$MM_p^2 M_5^4 r_0^3 - 4M^2 M_5^4 r_0^2 + 4MM_p^2 M_5^2 q r_0 - q^2 M_p^4 = 0 . \quad (3.36)$$

Let $r_0 = r_{mb}$ be the solution of the equation which gives the radius of MBCO of brane-world BH.

In the extremal limit the above Eq. reduces to

$$r_0^3 - 4r_+ r_0^2 + 4r_+^2 r_0 - r_+^3 = 0 . \quad (3.37)$$

or

$$r_0 = \left(\frac{3 + \sqrt{5}}{2} \right) r_+ = \left(\frac{3 + \sqrt{5}}{2} \right) \frac{M}{M_p^2} . \quad (3.38)$$

3.4 ISCO:

In astrophysics, there is an important class of orbit which is most relevant in accretion disk theory called ISCO or the orbit of marginal stability could be derived from the following criterion:

$$V_{eff} = \frac{dV_{eff}}{dr} = \frac{d^2 V_{eff}}{dr^2} = 0 \quad (3.39)$$

Thus one obtains

$$(r_+ + r_-)r_0^3 - 3(r_+ + r_-)^2 r_0^2 + 9r_+ r_- (r_+ + r_-)r_0 - 8(r_+ r_-)^2 = 0 . \quad (3.40)$$

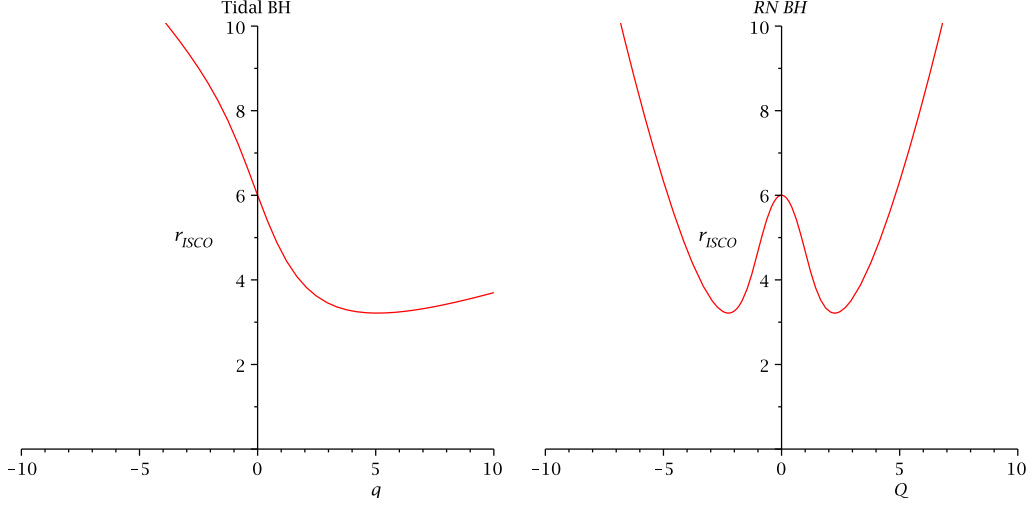


Figure 16. The figure shows the variation r_{ISCO} with charge parameter for RS tidal charged BH and RN BH with $M = M_p = M_5 = 1$.

or

$$MM_p^2M_5^4r_0^3 - 6M^2M_5^4r_0^2 + 9MM_p^2M_5^2qr_0 - 4q^2M_p^4 = 0. \quad (3.41)$$

Let $r_0 = r_{ISCO}$ be the solution of the equation which gives the radius of the ISCO:

$$\frac{r_{ISCO}}{M/M_p^2} = 2 + X^{1/3} + \frac{(4 - 3\frac{q}{M_5^2})}{X^{1/3}} \quad (3.42)$$

$$X = \left[8 - 9\left(\frac{qM_p^4}{M_5^2}M^2\right) + 2\frac{q^2M_p^8}{M^4M_5^4} + \sqrt{5\frac{q^2M_p^8}{M^4M_5^4} - 9\frac{q^3M_p^{12}}{M^6M_5^6} + 4\frac{q^4M_p^8}{M^8M_5^8}} \right]. \quad (3.43)$$

In Fig. 16 we show how the radius of ISCO changes with charge parameter both for brane-world BH and RN BH.

For extremal brane-world BH, one could obtain the ISCO equation reads

$$r_0^3 - 6r_+r_0^2 + 9r_+^2r_0 - 4r_+^3 = 0 \quad (3.44)$$

or

$$r_0 = 4r_+ = 4\frac{M}{M_p^2}. \quad (3.45)$$

4 CM Energy of Particle Collision near the horizon of the RS Tidal charged BH:

Now we shall calculate the CM energy of two particle collisions close to the horizon of the brane-world BH. To proceed, first we consider two particles are coming from infinity with $\frac{E_1}{m_\chi} = \frac{E_2}{m_\chi} = 1$ approaching the tidal charged BH with different angular momenta L_1 and

L_2 and colliding at some radius r . Later, we consider the collision point r to approach the horizon $r = r_+$. Also we have assumed that the particles to be at rest at infinity.

The CM energy is computed by using the following formula which was first derived by BSW [1] reads as

$$\left(\frac{E_{cm}}{\sqrt{2}m_\chi} \right)^2 = 1 - g_{\mu\nu} u_{(1)}^\mu u_{(2)}^\nu . \quad (4.1)$$

We shall also assume throughout the work, the geodesic motion of the colliding particles confined in the equatorial plane. Since the spacetime has a time-like isometry followed by the time-like Killing vector field ξ whose projection along the four velocity \mathbf{u} of geodesics $\xi \cdot \mathbf{u} = -E$, is conserved along such geodesics (where $\xi \equiv \partial_t$). Analogously, there is also the rotational symmetry for which the ‘angular momentum’ $L = \zeta \cdot \mathbf{u}$ is also conserved (where $\zeta \equiv \partial_\phi$).

Thus for massive particles, the components of the four velocity are

$$\dot{t} = \frac{E}{\mathcal{B}(r)} \quad (4.2)$$

$$\dot{r} = \dot{r} = \pm \sqrt{E^2 - \mathcal{B}(r) \left(1 + \frac{L^2}{r^2} \right)} \quad (4.3)$$

$$\dot{\theta} = 0 \quad (4.4)$$

$$\dot{\phi} = \frac{L}{r^2} . \quad (4.5)$$

and

$$u_{(1)}^\mu = \left(\frac{E_1}{\mathcal{B}(r)}, -X_1, 0, \frac{L_1}{r^2} \right) . \quad (4.6)$$

$$u_{(2)}^\mu = \left(\frac{E_2}{\mathcal{B}(r)}, -X_2, 0, \frac{L_2}{r^2} \right) . \quad (4.7)$$

In Figs. (17,18,19,20,21,22) we have plotted the radial component of the four velocity for various values of angular momentum for RS tidal charged BH in contrast with RN BH.

Substituting this in (4.1), we obtain the CM energy:

$$\left(\frac{E_{cm}}{\sqrt{2}m_\chi} \right)^2 = 1 + \frac{E_1 E_2}{\mathcal{B}(r)} - \frac{X_1 X_2}{\mathcal{B}(r)} - \frac{L_1 L_2}{r^2} . \quad (4.8)$$

where,

$$X_1 = \sqrt{E_1^2 - \mathcal{B}(r) \left(1 + \frac{L_1^2}{r^2} \right)}, \quad X_2 = \sqrt{E_2^2 - \mathcal{B}(r) \left(1 + \frac{L_2^2}{r^2} \right)}$$

For simplicity, we have taken $E_1 = E_2 = 1$ and substituting the value of $\mathcal{B}(r)$,

Case I: when $q \geq 0$, we get the CM energy near the event horizon (r_+) of the tidal charged BH:

$$E_{cm} |_{r \rightarrow r_+} = \sqrt{2}m_\chi \sqrt{2 + (L_1 - L_2)^2 \frac{M_p^2 M_5^2}{2(2MM_5^2 r_+ - qM_p^2)}} . \quad (4.9)$$

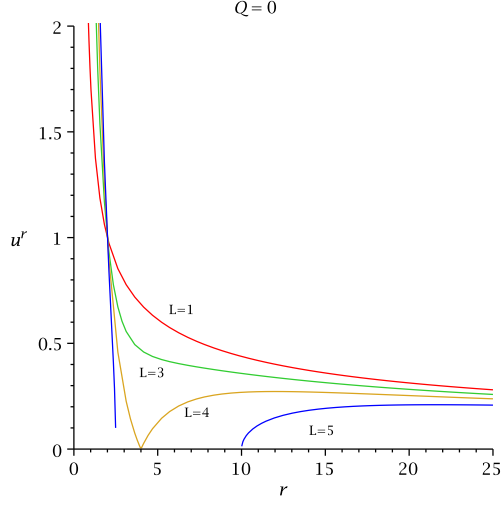


Figure 17. The figure shows the variation of \dot{r} with r for RS tidal charged BH in the limit $q = 0$ with $M = M_p = M_5 = 1$.

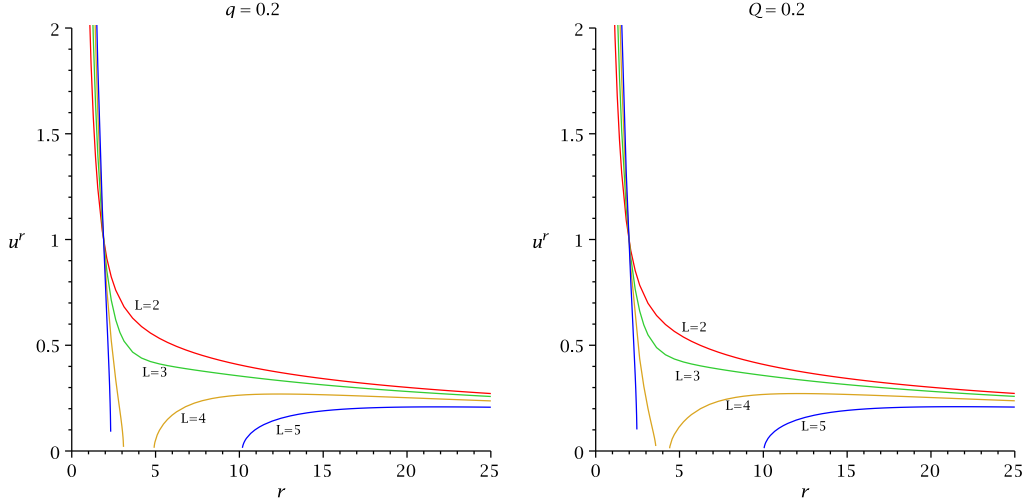


Figure 18. The figure shows the variation of \dot{r} with r for RS tidal charged BH and RN BH with $M = M_p = M_5 = 1$.

and near the Cauchy horizon (r_-) is given by

$$E_{cm} |_{r \rightarrow r_-} = \sqrt{2} m_\chi \sqrt{2 + (L_1 - L_2)^2 \frac{M_p^2 M_5^2}{2(2M M_5^2 r_- - q M_p^2)}}. \quad (4.10)$$

Which shows that the CM energy is finite and depend upon the values of the angular momentum parameter.

Case II: When $q < 0$, which gives the single horizon r_+ described by Eq. (2.10) lying

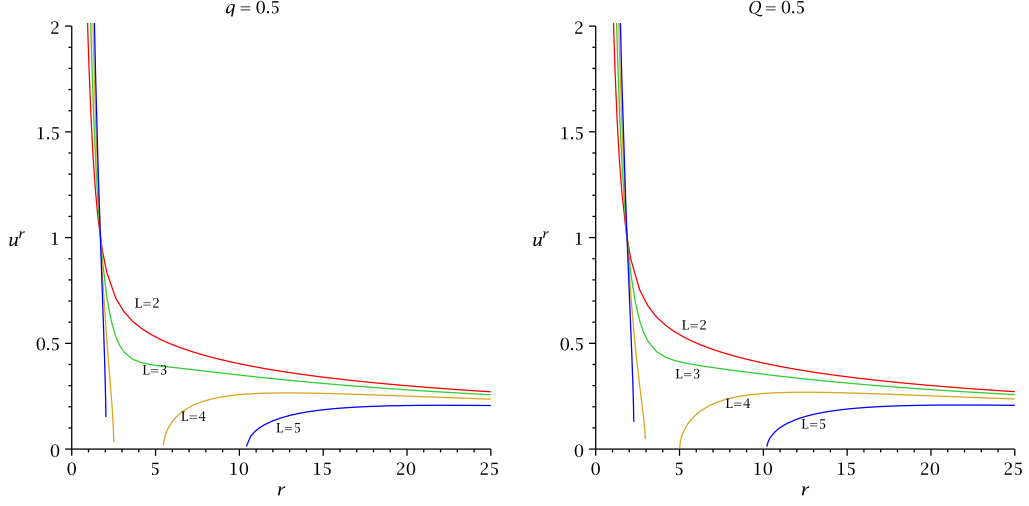


Figure 19. The figure shows the variation of \dot{r} with r for RS tidal charged BH and RN BH with $M = M_p = M_5 = 1$.

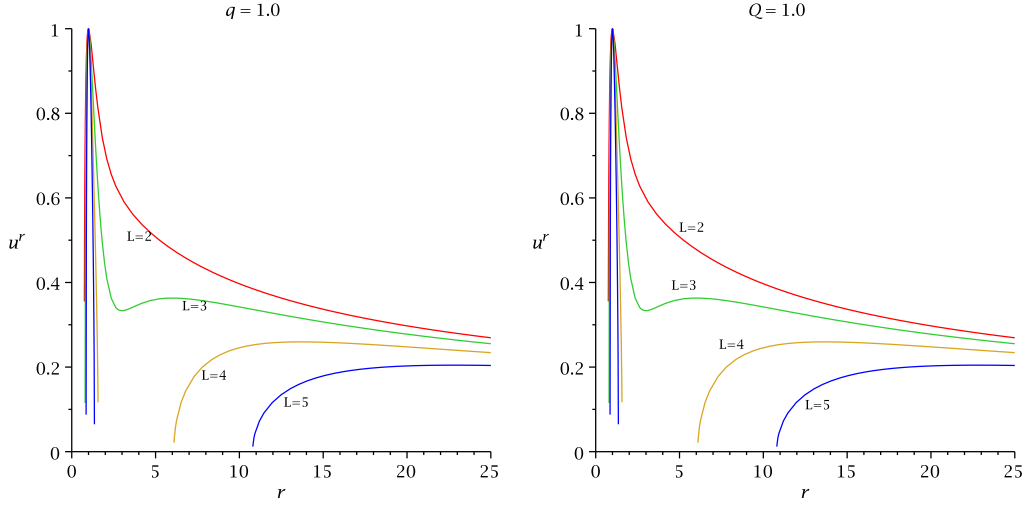


Figure 20. The figure shows the variation of \dot{r} with r for RS tidal charged BH and RN BH with $M = M_p = M_5 = 1$.

exterior to the Schwarzschild horizon and thus the CM energy in this case is

$$E_{cm} |_{r \rightarrow r_+} = \sqrt{2} m_\chi \sqrt{2 + (L_1 - L_2)^2 \frac{M_p^2 M_5^2}{2(2MM_5^2 r_+ - qM_p^2)}}. \quad (4.11)$$

and which is also finite and depends upon the angular momentum parameter.

Case III: For $M = 0$ and $q < 0$, we get the CM energy is given by

$$E_{cm} |_{r \rightarrow r_+} = \sqrt{2} m_\chi \sqrt{2 - (L_1 - L_2)^2 \frac{M_5^2}{2q}}. \quad (4.12)$$

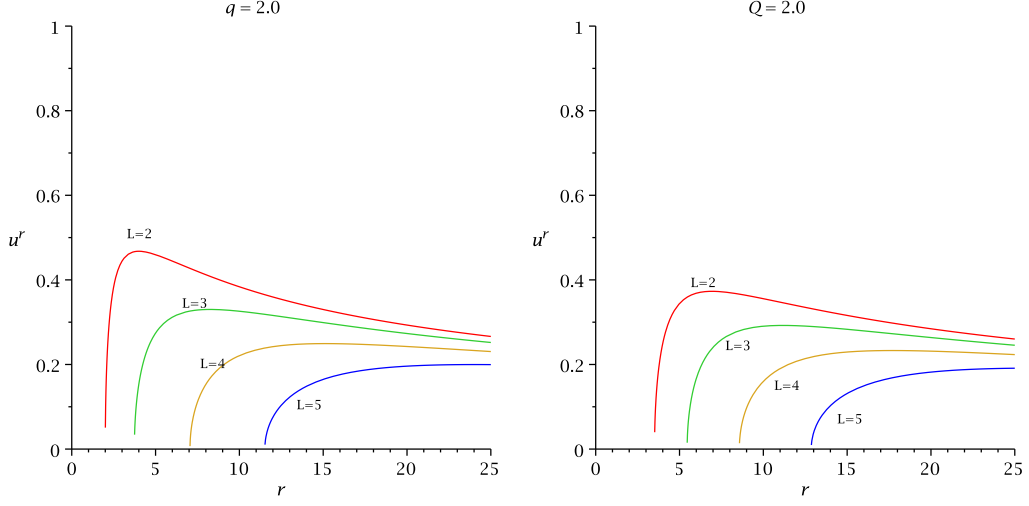


Figure 21. The figure shows the variation of \dot{r} with r for RS tidal charged BH and RN BH with $M = M_p = M_5 = 1$.

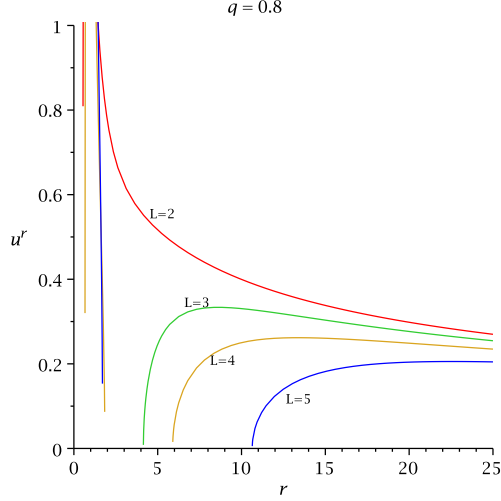


Figure 22. The figure shows the variation of \dot{r} with r for RS tidal charged BH and RN BH with $M = M_p = M_5 = 1$.

This is also a finite quantity.

In Figs. (23,24,25,26,27,28,29,30,31) we show how the CM energy E_{cm} changes in case of RS tidal charged BH with the radial coordinate r for various combination of angular momentum parameters L_1 and L_2 .

It was discussed in[1] that the maximum CM energy strictly depend upon the values of critical angular momentum such that the particles can reach the outer horizon with maximum tangential velocity. Therefore the critical angular momentum and the critical radius could be derived from the radial effective potential. Now we impose the following

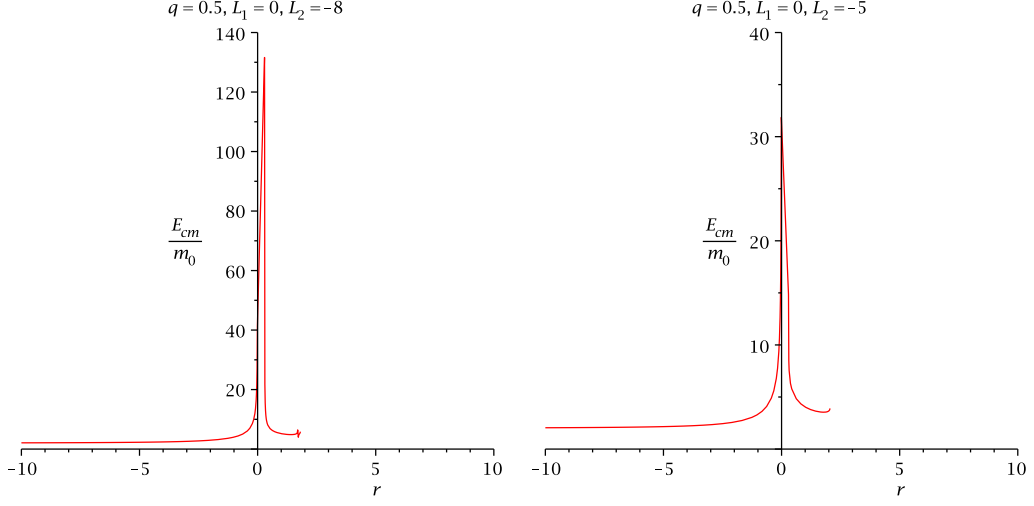


Figure 23. The figure shows the variation of E_{cm} with r for RS tidal charged BH with $M = M_p = M_5 = 1$.

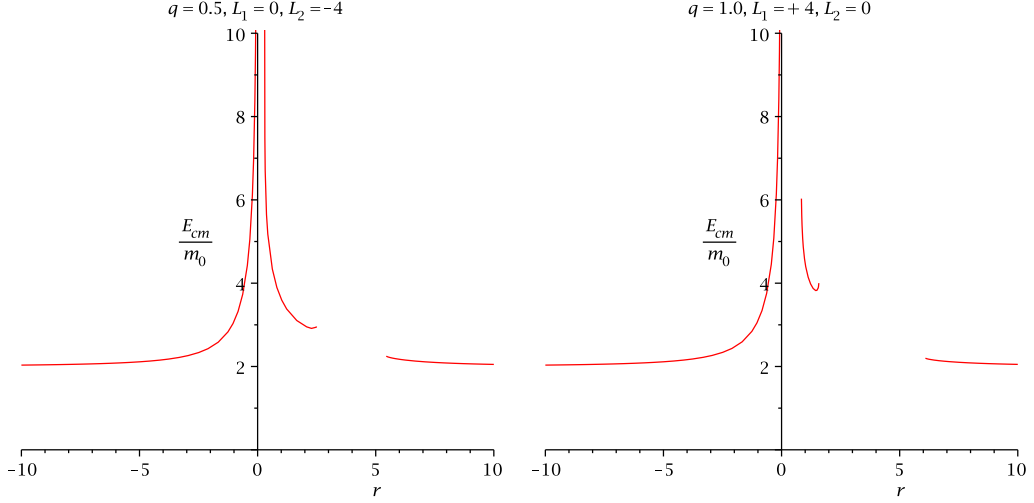


Figure 24. The figure shows the variation of E_{cm} with r for RS tidal charged BH with $M = M_p = M_5 = 1$.

condition for determining the critical values of angular momentum i.e. :

$$r^2 r^4 = (E^2 - 1)r^4 + 2\frac{M}{M_p^2}r^3 - (L^2 + \frac{q}{M_5^2})r^2 + 2\frac{M}{M_p^2}L^2r - \frac{q}{M_5^2}L^2 = 0 . \quad (4.13)$$

Now setting $E^2 = 1$ for marginal case, the equation turns out to be

$$2\frac{M}{M_p^2}r^3 - (L^2 + \frac{q}{M_5^2})r^2 + 2\frac{M}{M_p^2}L^2r - \frac{q}{M_5^2}L^2 = 0 . \quad (4.14)$$

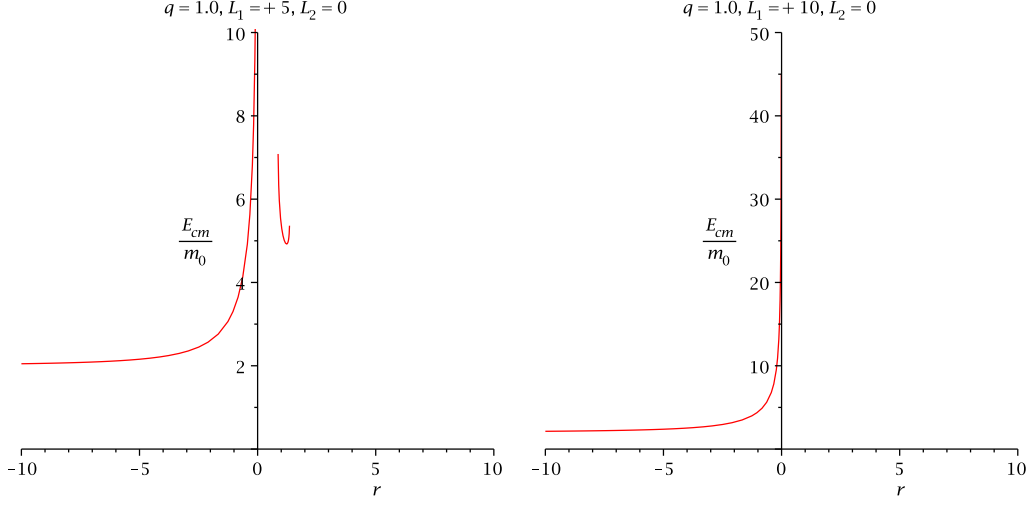


Figure 25. The figure shows the variation of E_{cm} with r for RS tidal charged BH with $M = M_p = M_5 = 1$.

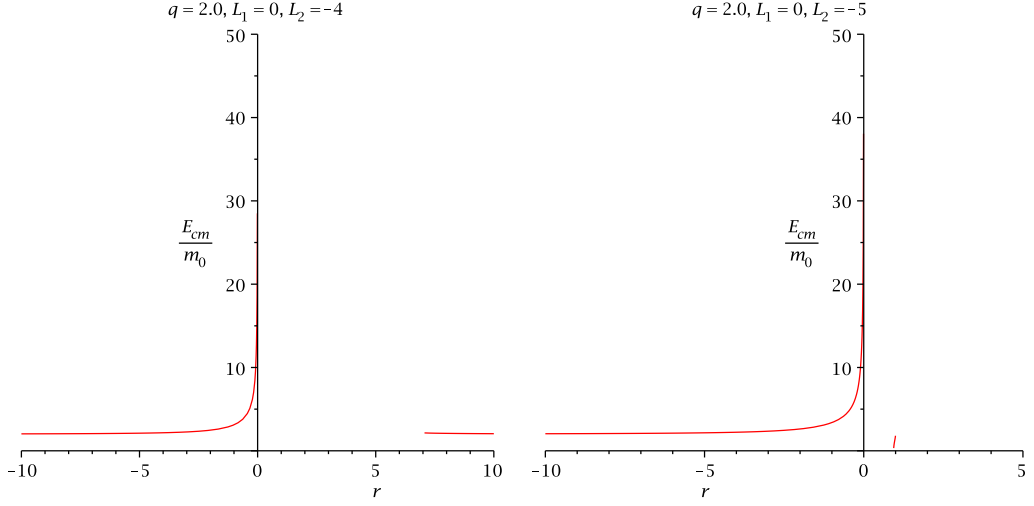


Figure 26. The figure shows the variation of E_{cm} with r for RS tidal charged BH with $M = M_p = M_5 = 1$.

For non-extremal tidal charged BH, one could obtain the critical values of angular momentum by solving the following equation:

$$\left(\frac{M^2}{M_p^4} - \frac{q}{M_5^2}\right)L^6 - \left(3\frac{q^2}{M_5^4} - 20\frac{M^2}{M_p^4}\frac{q}{M_5^2} + 16\frac{M^4}{M_p^8}\right)L^4 - \left(8\frac{M^2}{M_p^4} + 3\frac{q}{M_5^2}\right)\frac{q^2}{M_5^4}L^2 - \frac{q^4}{M_5^8} = 0 \quad (4.15)$$

In the limit $q = 0$, we obtain the critical values of angular momentum for Schwarzschild BH:

$$L = \pm 4 \frac{M}{M_p^2} . \quad (4.16)$$

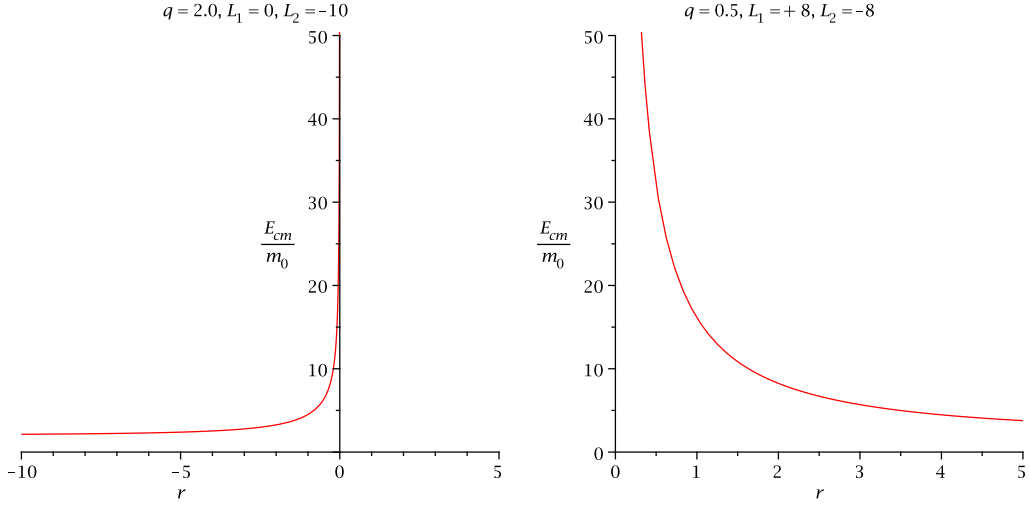


Figure 27. The figure shows the variation of E_{cm} with r for RS tidal charged BH with $M = M_p = M_5 = 1$.

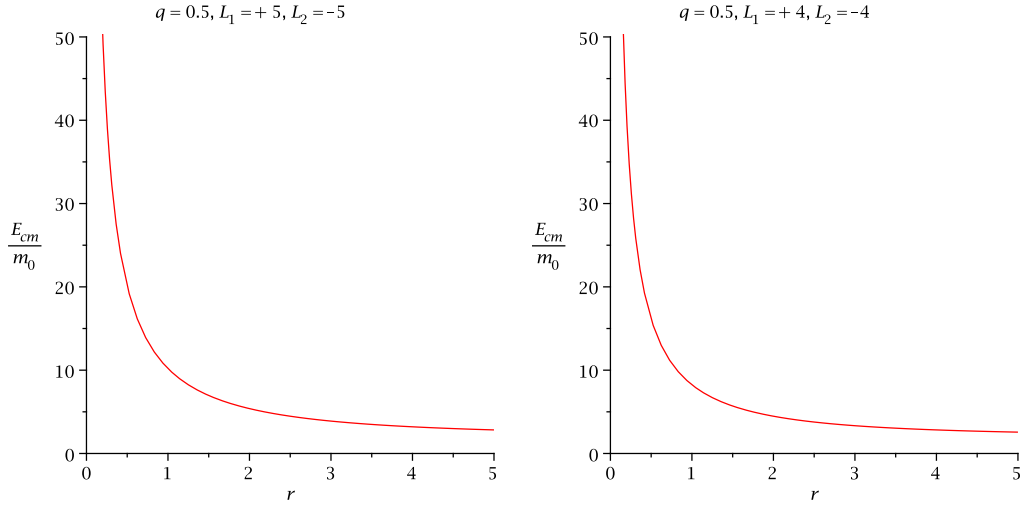


Figure 28. The figure shows the variation of E_{cm} with r for RS tidal charged BH with $M = M_p = M_5 = 1$.

For extremal RS tidal charged BH, it could be easily obtained the regime of the angular momentum L for in-falling geodesics:

$$-\sqrt{\frac{11+5\sqrt{5}}{2}} \frac{M}{M_p^2} \leq L \leq \sqrt{\frac{11+5\sqrt{5}}{2}} \frac{M}{M_p^2} . \quad (4.17)$$

For extremal RS tidal charged BH, the values of CM energy near the horizon is given

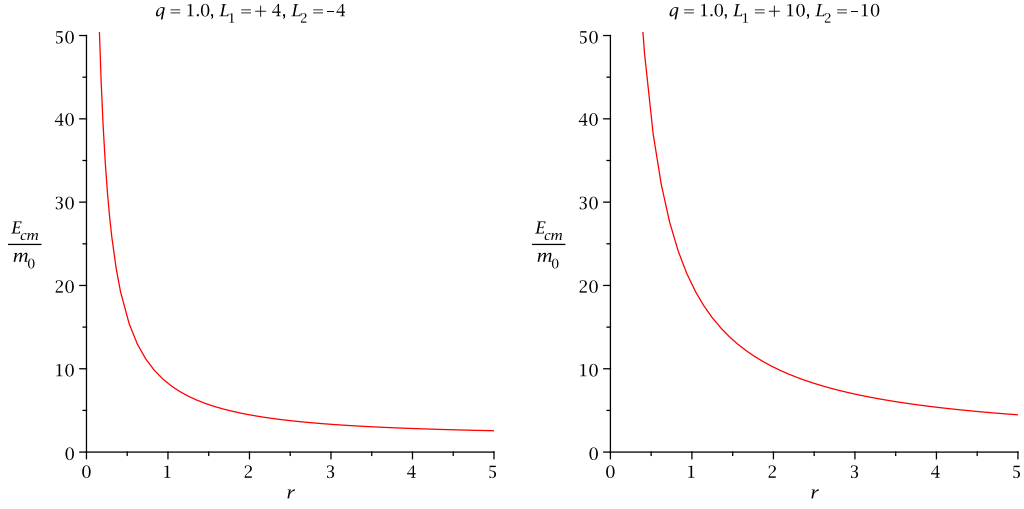


Figure 29. The figure shows the variation of E_{cm} with r for RS tidal charged BH with $M = M_p = M_5 = 1$.

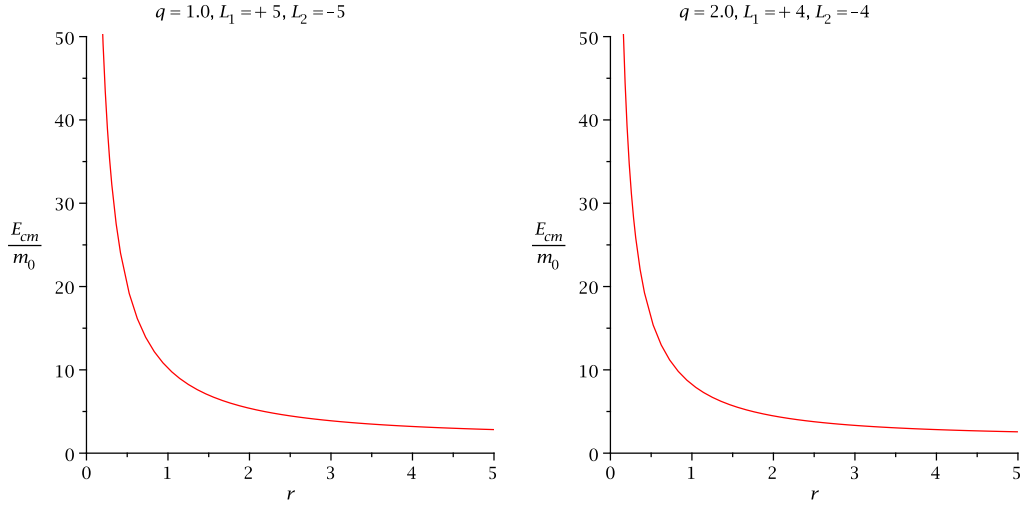


Figure 30. The figure shows the variation of E_{cm} with r for RS tidal charged BH with $M = M_p = M_5 = 1$.

by

$$E_{cm} \big|_{r \rightarrow \frac{M}{M_p^2}} = \sqrt{2} m_\chi \sqrt{\frac{4 \frac{M^2}{M_p^4} + (L_1 - L_2)^2}{2 \frac{M^2}{M_p^4}}} . \quad (4.18)$$

Since here we have chosen the collision point is at $r = \frac{M}{M_p^2}$ and two particles have the

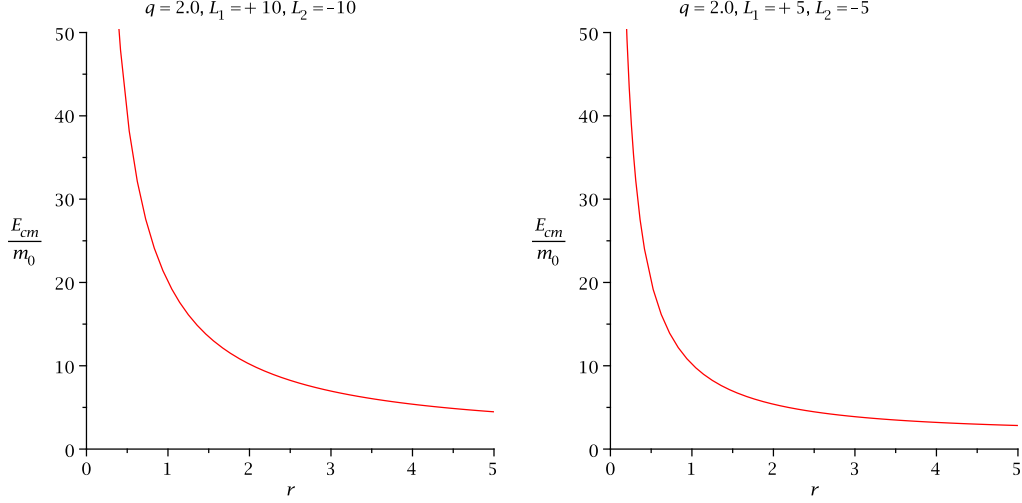


Figure 31. The figure shows the variation of E_{cm} with r for RS tidal charged BH with $M = M_p = M_5 = 1$.

angular momentum which is given by the following equation:

$$L = \pm \sqrt{\frac{r^2(2\frac{M}{M_p^2}r - \frac{q}{M_5^2})}{r^2 - 2\frac{M}{M_p^2}r + \frac{q}{M_5^2}}} \quad (4.19)$$

In the extremal limit, it goes to

$$L = \pm \sqrt{\frac{\frac{M}{M_p^2}r^2(2r - \frac{M}{M_p^2})}{(r - \frac{M}{M_p^2})^2}} \quad (4.20)$$

It has been already mentioned in [1], a new process would be appear if one of the particles participating in the collision has the critical angular momentum. If one of the particles have the diverging angular momentum at the horizon i.e.

$$L_1 \big|_{r=\frac{M}{M_p^2}} = \sqrt{\frac{\frac{M}{M_p^2}r^2(2r - \frac{M}{M_p^2})}{(r - \frac{M}{M_p^2})^2}} \rightarrow \infty \quad (4.21)$$

then the corresponding value of the CM energy for extremal RS tidal charged BH at the extremal horizon is

$$E_{cm} \big|_{r \rightarrow \frac{M}{M_p^2}} = \sqrt{2}m_\chi \sqrt{\frac{4\frac{M^2}{M_p^4} + (L_1 - L_2)^2}{2\frac{M^2}{M_p^4}}} \rightarrow \infty \quad (4.22)$$

Thus for the extremal RS tidal charged BH, we obtain the infinite amounts of CM energy.

Now let us check, what will be the CM energy if we choose the collision point to be ISCO? We have already been derived in the previous section the ISCO which is occur at

$r = 4\frac{M}{M_p^2}$ for extremal RS tidal charged BH. Thus the CM energy at ISCO is given by

$$E_{cm} \big|_{r \rightarrow 4\frac{M}{M_p^2}} = \sqrt{2}m_\chi \sqrt{\frac{400\frac{M^2}{M_p^4} - 9L_1L_2 - \sqrt{112\frac{M^2}{M_p^4} - 9L_1^2}\sqrt{112\frac{M^2}{M_p^4} - 9L_2^2}}{144\frac{M^2}{M_p^4}}} . \quad (4.23)$$

For the critical values of angular momentum $L_1 = \sqrt{\frac{11+5\sqrt{5}}{2}}\frac{M}{M_p^2}$ and $L_2 = -\sqrt{\frac{11+5\sqrt{5}}{2}}\frac{M}{M_p^2}$, the CM energy is found to be

$$E_{cm} \big|_{r \rightarrow 4\frac{M}{M_p^2}} = \sqrt{2}m_\chi \sqrt{\frac{387 + 45\sqrt{5}}{144}} = 2.60m_\chi \quad (4.24)$$

Similarly, one may compute the MBCO for RS tidal charged BH by setting $E_0^2 = 1$ which turns out to be $r_{mb} = \left(\frac{3+\sqrt{5}}{2}\right)\frac{M}{M_p^2}$. Thus when the collision point to be MBCO, the CM energy is found to be at $r = r_{mb}$:

$$E_{cm} \big|_{r \rightarrow r_{mb}} = \sqrt{2}m_\chi \sqrt{\frac{(10 + 4\sqrt{5})(7 + 3\sqrt{5})\frac{M^2}{M_p^4} - (6 + 2\sqrt{5})L_1L_2 - \Upsilon_1\Upsilon_2}{(3 + \sqrt{5})(7 + 3\sqrt{5})\frac{M^2}{M_p^4}}} . \quad (4.25)$$

where

$$\Upsilon_1 = \sqrt{(58 + 26\sqrt{5})\frac{M^2}{M_p^4} - (6 + 2\sqrt{5})L_1^2} \quad (4.26)$$

$$\Upsilon_2 = \sqrt{(58 + 26\sqrt{5})\frac{M^2}{M_p^4} - (6 + 2\sqrt{5})L_2^2} \quad (4.27)$$

For the critical values of angular momentum $L_1 = \sqrt{\frac{11+5\sqrt{5}}{2}}\frac{M}{M_p^2}$ and $L_2 = -\sqrt{\frac{11+5\sqrt{5}}{2}}\frac{M}{M_p^2}$, the CM energy is at r_{mb} found to be

$$E_{cm} \big|_{r=r_{mb}} = \sqrt{2}m_\chi \sqrt{\frac{47 + 21\sqrt{5}}{9 + 4\sqrt{5}}} = 3.23m_\chi \quad (4.28)$$

Now we can compare the results obtained as

$$E_{cm} \big|_{r_+ = \frac{M}{M_p^2}} : E_{cm} \big|_{r_{mb} = \left(\frac{3+\sqrt{5}}{2}\right)\frac{M}{M_p^2}} : E_{cm} \big|_{r_{ISCO} = 4\frac{M}{M_p^2}} = \infty : 3.23 : 2.6. \quad (4.29)$$

Thus we get,

$$E_{cm} \big|_{r_+} > E_{cm} \big|_{r_{mb}} > E_{cm} \big|_{r_{ISCO}} . \quad (4.30)$$

It is clearly evident that CM energy is diverging at the event horizon and finite at the MBCO and at ISCO.

In the limit $L_1 = L_2 = 0$, we obtain the following equality:

$$E_{cm} \big|_{r_+} = E_{cm} \big|_{r_{mb}} = E_{cm} \big|_{r_{ISCO}} = 2m_\chi. \quad (4.31)$$

It should be noted that in the limit $q \rightarrow 0$, the above expression reduces to

$$E_{cm} = \sqrt{2}m_\chi \sqrt{\frac{16\frac{M^2}{M_p^4} + (L_1 - L_2)^2}{8\frac{M^2}{M_p^4}}} . \quad (4.32)$$

which is the CM energy of the Schwarzschild BH. In fact this is indeed a finite quantity which was first observed in [1].

For our completeness, we have to derived the CM energy shortly for RN BH in the next section.

5 CM Energy of Particle Collision near the Horizon of a non-Extremal RN BH:

The well known metric for RN space-time can be written as

$$ds^2 = -\mathcal{A}(r)dt^2 + \frac{dr^2}{\mathcal{A}(r)} + r^2 (d\theta^2 + \sin^2 \theta d\phi^2) . \quad (5.1)$$

where the function $\mathcal{A}(r)$ is defined by

$$\mathcal{A}(r) = \left(1 - \frac{r_+}{r}\right) \left(1 - \frac{r_-}{r}\right) . \quad (5.2)$$

The BH has event horizon which is situated at $r_+ = M + \sqrt{M^2 - Q^2}$ and Cauchy horizon which is situated at $r_- = M - \sqrt{M^2 - Q^2}$. The equatorial time-like geodesics of RN BHs are

$$u^t = \frac{E}{\mathcal{A}(r)} \quad (5.3)$$

$$u^r = \pm \sqrt{E^2 - \mathcal{A}(r) \left(1 + \frac{L^2}{r^2}\right)} \quad (5.4)$$

$$u^\theta = 0 \quad (5.5)$$

$$u^\phi = \frac{L}{r^2} . \quad (5.6)$$

Next, we compute the CM energy for the RN space-time by using the well known formula as given by Bañados et al. in [1]:

$$\left(\frac{E_{cm}}{\sqrt{2}m_\chi}\right)^2 = 1 - g_{\mu\nu}u_{(1)}^\mu u_{(2)}^\nu . \quad (5.7)$$

where $u_{(1)}^\mu$ and $u_{(2)}^\nu$ are the four velocity of the two particles, which can be found from the following equation(5.6).

$$u_{(1)}^\mu = \left(\frac{E_1}{\mathcal{A}(r)}, -Y_1, 0, \frac{L_1}{r^2}\right) . \quad (5.8)$$

$$u_{(2)}^\mu = \left(\frac{E_2}{\mathcal{A}(r)}, -Y_2, 0, \frac{L_2}{r^2}\right) . \quad (5.9)$$

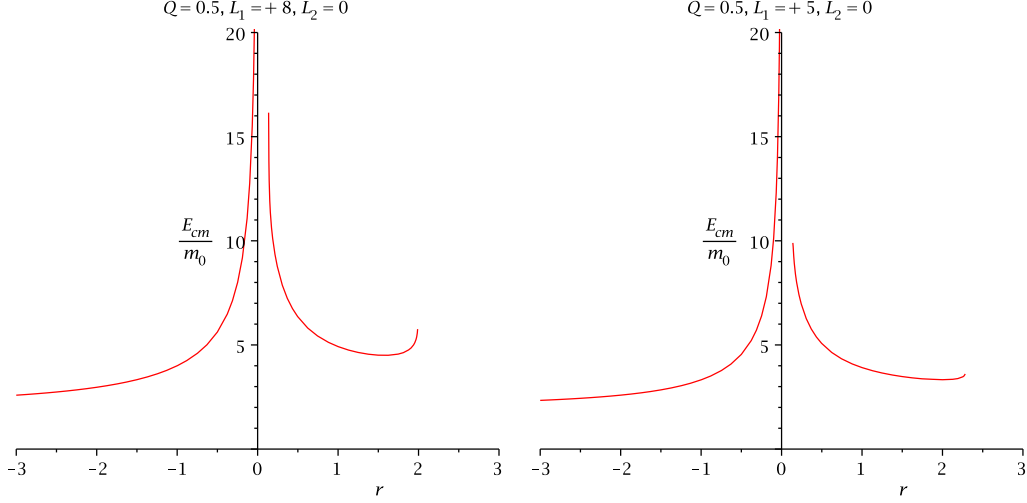


Figure 32. The figure shows the variation of E_{cm} with r for RN BH with $M = 1$.

Therefore using (5.7) one can obtain the center-of-mass energy for this collision:

$$\left(\frac{E_{cm}}{\sqrt{2}m_\chi} \right)^2 = 1 + \frac{E_1 E_2}{\mathcal{A}(r)} - \frac{Y_1 Y_2}{\mathcal{A}(r)} - \frac{L_1 L_2}{r^2}. \quad (5.10)$$

$$\text{where} \quad (5.11)$$

$$Y_1 = \sqrt{E_1^2 - \mathcal{A}(r) \left(1 + \frac{L_1^2}{r^2} \right)}$$

$$Y_2 = \sqrt{E_2^2 - \mathcal{A}(r) \left(1 + \frac{L_2^2}{r^2} \right)} \quad (5.12)$$

As we have assumed $E_1 = E_2 = 1$ previously, and substituting the value of $\mathcal{A}(r)$ one could obtain finally the CM energy near the event horizon(r_+) for non-extremal RN space-time

$$E_{cm} |_{r \rightarrow r_+} = \sqrt{2}m_\chi \sqrt{\frac{4r_+^2 + (L_1 - L_2)^2}{2r_+^2}}. \quad (5.13)$$

Figs. (32,33,34,35,36,37,38,39,40,41) demonstrates the variation of CM energy with radial coordinate r for various combination of angular momentum parameters L_1 and L_2 for RN BH.

Analogously, the critical values of angular momentum parameter for extremal RN BH is given by

$$-\sqrt{\frac{11 + 5\sqrt{5}}{2}}M \leq L \leq \sqrt{\frac{11 + 5\sqrt{5}}{2}}M \quad (5.14)$$

which is exactly same as extremal RS tidal charged BH.

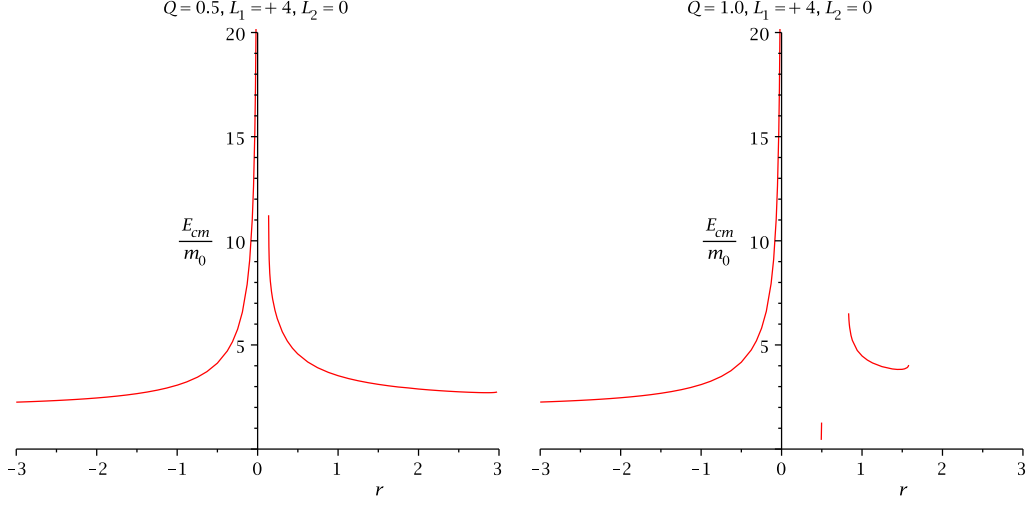


Figure 33. The figure shows the variation of E_{cm} with r for RN BH with $M = 1$.

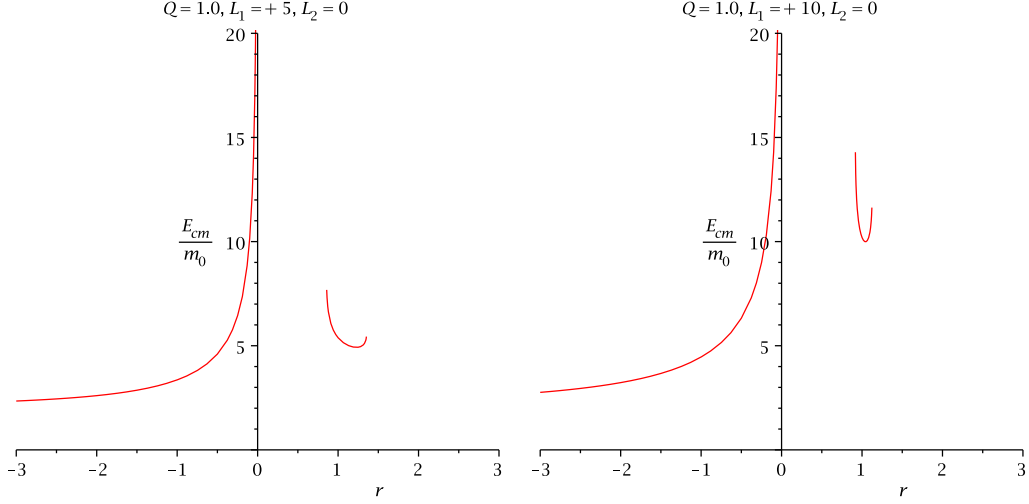


Figure 34. The figure shows the variation of E_{cm} with r for RN BH with $M = 1$.

Thus for extremal RN space-time, the values of CM energy near the horizon is given by

$$E_{cm} |_{r \rightarrow M} = \sqrt{2} m_\chi \sqrt{\frac{4M^2 + (L_1 - L_2)^2}{2M^2}}. \quad (5.15)$$

Thus we get the CM energy for extreme RN BH is diverging due to one of the two particles have diverging angular momentum at the horizon. Therefore,

$$E_{cm} |_{r \rightarrow M} = \sqrt{2} m_\chi \sqrt{\frac{4M^2 + (L_1 - L_2)^2}{2M^2}} \rightarrow \infty. \quad (5.16)$$

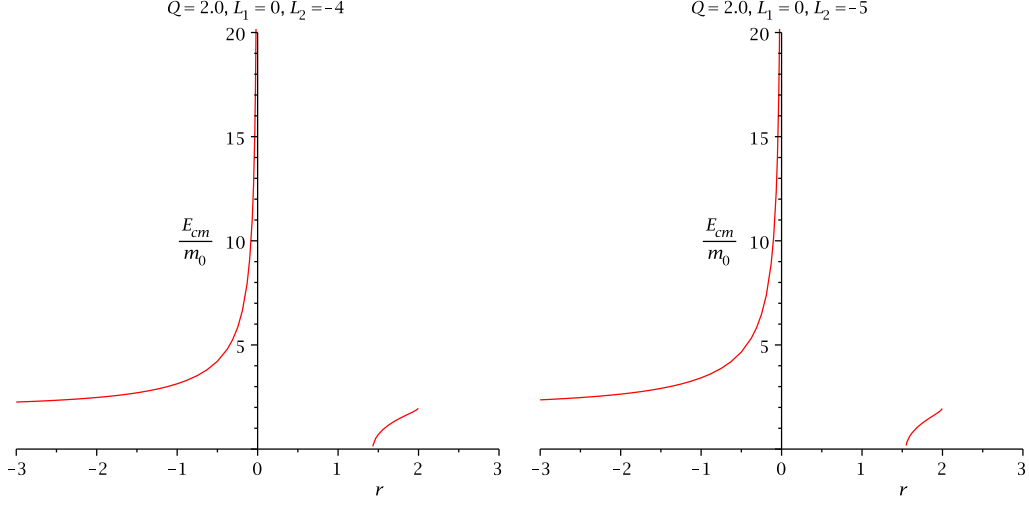


Figure 35. The figure shows the variation of E_{cm} with r for RN BH with $M = 1$.

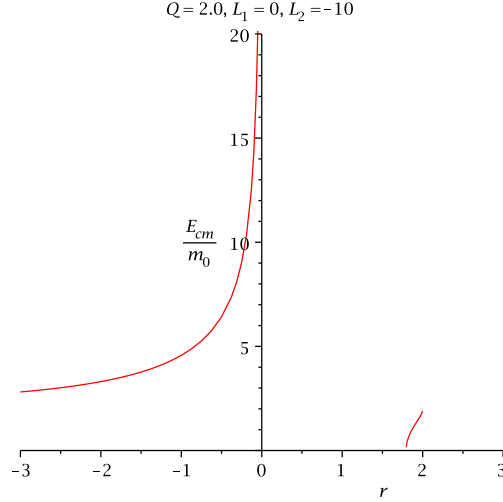


Figure 36. The figure shows the variation of E_{cm} with r for RN BH with $M = 1$.

6 Summary and Outlook:

In this work, we have investigated the BSW effect for RS tidal charged BH. Firstly, we have given the detailed treatment of geodesics of the said BHs both time-like case as well as light-like case. ISCO, MBCO and CPO of the said BHs are also calculated. We have shown graphically the qualitative difference in the geodesic structure between RS tidal BH and RN BH. In the extremal cases, we found their properties are same. Then we have computed the CM energy both for non-extremal and extremal cases. We have found the CM energy is finite for non-extremal case and it is infinite for extremal cases. We have also shown that for extreme RS tidal charged BH the CM energy is diverging at the

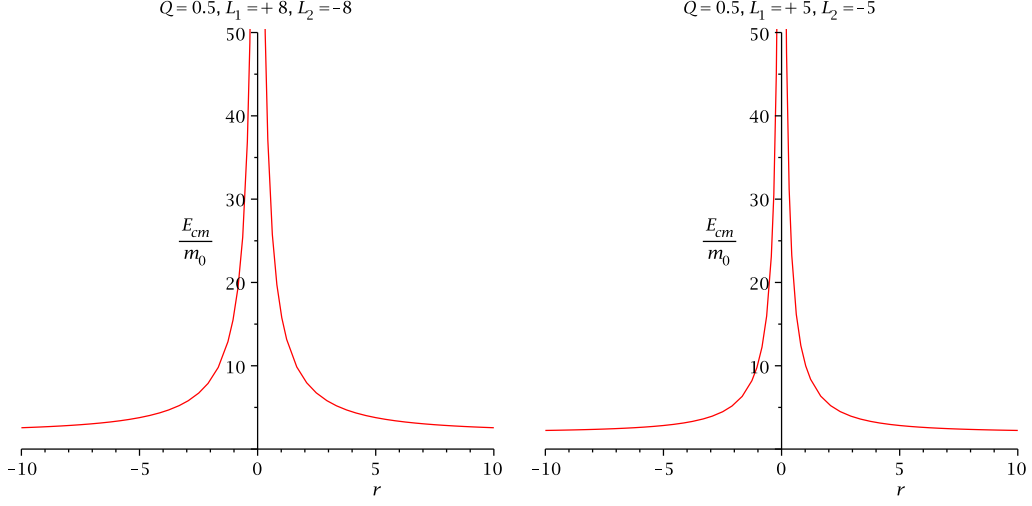


Figure 37. The figure shows the variation of E_{cm} with r for RN BH with $M = 1$.

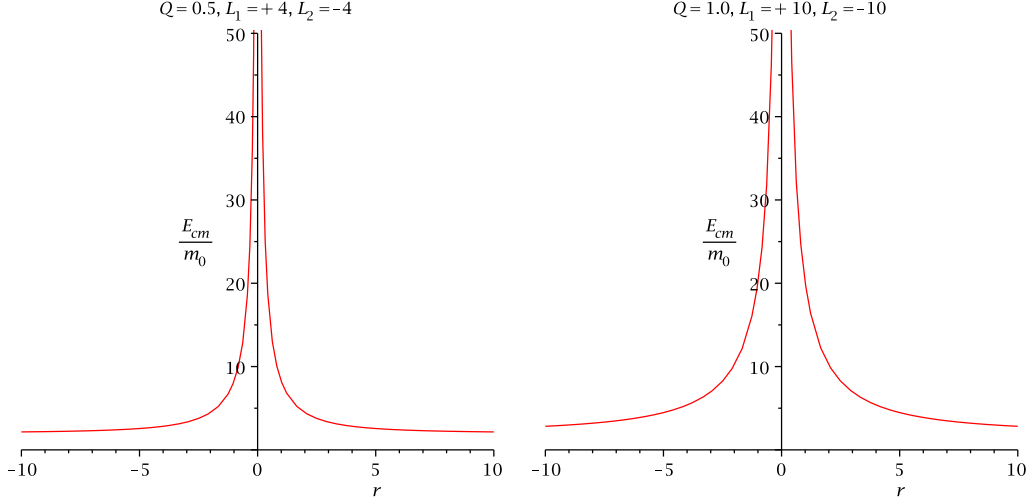


Figure 38. The figure shows the variation of E_{cm} with r for RN BH with $M = 1$.

extremal horizon and finite at the MBCO and ISCO. Their ratio varies as $E_{cm} \big|_{r_+=\frac{M}{M_p^2}} : E_{cm} \big|_{r_{mb}=\left(\frac{3+\sqrt{5}}{2}\right)\frac{M}{M_p^2}} : E_{cm} \big|_{r_{ISCO}=4\frac{M}{M_p^2}} = \infty : 3.23 : 2.6$. Which is exactly similar to the extremal RN BH. When tidal charge goes to zero i.e. Schwarzschild BH[28] the ratio of CM energy is $E_{cm} \big|_{r_+=2M} : E_{cm} \big|_{r_{mb}=4M} : E_{cm} \big|_{r_{ISCO}=6M} = \sqrt{5} : \sqrt{2} : \frac{\sqrt{13}}{3}$.

References

- [1] M. Bañados, J. Silk, and S. M. West, *Phys. Rev. Lett.* **103**, 111102 (2009).
- [2] A. N. Baushev, *Int. J. Mod. Phys. D* **18**, 1195 (2009).

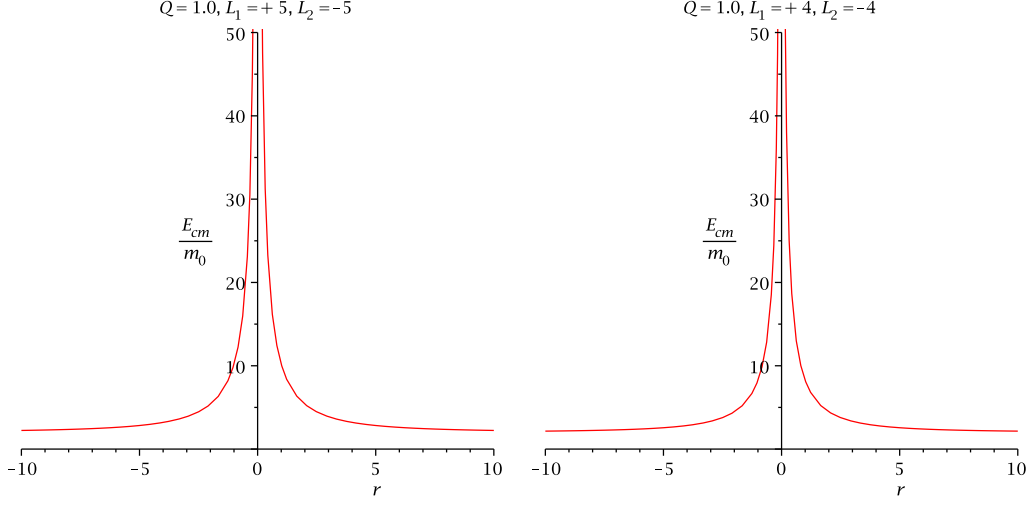


Figure 39. The figure shows the variation of E_{cm} with r for RN BH with $M = 1$.

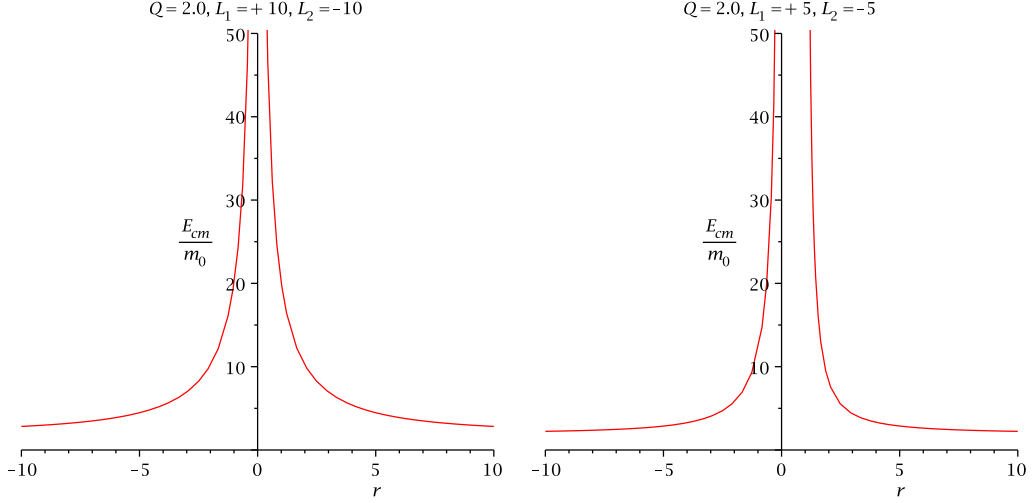


Figure 40. The figure shows the variation of E_{cm} with r for RN BH with $M = 1$.

- [3] M. Bañados, B. Hassanain, J. Silk, and S. M. West, *Phys. Rev. D.* **83**, 023004 (2011).
- [4] E. Berti, V. Cardoso, L. Gualtieri, F. Pretorius, and U. Sperhake, *Phys. Rev. Lett.* **103**, 239001 (2009).
- [5] T. Jacobson and T. P. Sotiriou, *Phys. Rev. Lett.* **104**, 021101 (2010).
- [6] K. S. Thorn, *Astrophys. J.* **191**, 507 (1974).
- [7] M. Bejger, T. Piran, M. Abramowicz, and F. Håkanson, *Phys. Rev. Lett.* **109**, 121101 (2012).
- [8] J. D. Schnittman, arXiv:1410.6446[astro-ph].
- [9] E. Berti, R. Brito and V. Cardoso, arXiv:1410.8534[gr-qc].

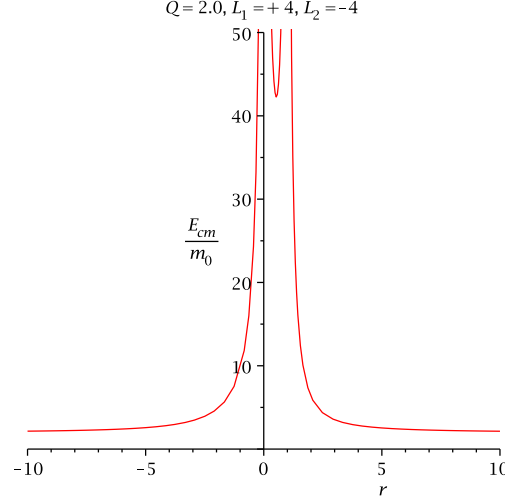


Figure 41. The figure shows the variation of E_{cm} with r for RN BH with $M = 1$.

- [10] K. Lake, *Phys. Rev. Lett.* **104**, 211102 (2010) [Erratum-ibid. **104**, 259903 (2010)].
- [11] A. Grib, Y. Pavlov, *Astropart. Phys.* **34**, 581 (2011).
- [12] A. Grib, Y. Pavlov, *Euro. Phys. Lett.* **101**, 20004 (2013).
- [13] T. Harada, M. Kimura, *Phys. Rev. D* **83**, 024002(2011).
- [14] C. Liu, S. Chen, C. Ding, J. Jing, *Phys. Letters B* **701**, 285-290 (2011).
- [15] Y. Li, J. Yang, Y. Li, S. Wei, Y. Liu, *Class. Quant. Grav.* **28**, 225006 (2011).
- [16] C. Zhong, S. Gao, *JETP Letters* **94**, 589 (2011).
- [17] J. L. Said, K. Z. Adami, *Phys. Rev. D* **83**, 104047 (2011).
- [18] M. Patil, P. Joshi, *Phys. Rev. D* **85**, 104014 (2012); A. N. Chowdhury, M. Patil, D. Malafarina, P. S. Joshi, *Phys. Rev. D* **85**, 104031 (2012).
- [19] S. W. Wei, Y. X. Liu, H. Guo, C. E. Fu, *Phys. Rev. D* **82**, 103005 (2010).
- [20] S. Wei, Y. Liu, H. Li, F. Chen, *JHEP* **1012**, 066 (2010).
- [21] O. Zaslavskii, *JETP Lett.* **92**, 571, (2010).
- [22] Y. Zhu, S. Wu, Y. Jiang, G. Yang, *Phys. Rev. D* **84**, 123002, 043006 (2011).
- [23] V. P. Frolov, *Phys. Rev. D* **86**, 044040 (2012).
- [24] S. Mc Williams, *Phys. Rev. Lett.* **110**, 011102 (2012).
- [25] A. Galajinsky, *Phys. Rev. D* **88**, 027505 (2013).
- [26] A. Tursunov, M. Kološ, A. Abdujabbarov, B. Ahmedov and Z. Stuchlík, *Phys. Rev. D*, **88**, 124001 (2013).
- [27] P. Pradhan, *Astrophys Space Sci.*, DOI: 10.1007/s 10509-014-1896-9.
- [28] P. Pradhan, *Astroparticle Physics* **62**, 217-229 (2015).

- [29] S. Chandrashekar, *The Mathematical Theory of Black Holes*, Clarendon Press, Oxford (1983).
- [30] N. Arkani-Hamed, S. Dimopoulos, and G. Dvali, *Phys. Letters B* **429**, 263, (1998).
- [31] I. Antoniadis, N. Arkani-Hamed, S. Dimopoulos, and G. Dvali, *Phys. Letters B* **436**, 257, (1998).
- [32] L. Randall and R. Sundrum, *Phys. Rev. Lett.* **83**, 4690 (1999).
- [33] N. Dadhich, R. Maartens, P. Papadopoulos, and V. Rezanian, *Phys. Letters B* **487**, 1, (2000).
- [34] S. Dimopoulos and G. Landsberg, *Phys. Rev. Lett.* **87**, 161602(2001).
- [35] R. Casadio, S. Fabi, B. Harms, and O. Micu, *JHEP* **02**, 79 (2010).
- [36] D. M. Gingrich, *Phys. Rev. D* **81**, 057702(2010).
- [37] L. A. Gergely, N. Pidokrajt and S. Winitzki, *Eur. Phys. J. C* **71**, 1569 (2011).